

M. Tech Structural Engineering

Shashwat Vashistha

2023

**CFD ANALYSIS FOR WIND FLOW CHARACTERISTICS  
OF VARIOUS FACES IN AN H-SHAPED TALL BUILDING  
USING ANSYS CFX**

A DISSERTATION

SUBMITTED IN PARTIAL FULFILLMENT OF THE  
REQUIREMENTS FOR THE AWARD OF THE DEGREE OF

MASTER OF TECHNOLOGY

IN

**STRUCTURAL ENGINEERING**

Submitted by:

**SHASHWAT VASHISTHA**

**(2K21/STE/19)**

Under the supervision of

**DR. RITU RAJ AHIRWAR**

**Assistant Professor**



**DEPARTMENT OF CIVIL ENGINEERING**

**DELHI TECHNOLOGICAL UNIVERSITY**

(Formerly Delhi College of Engineering)

Bawana Road, Delhi-110042

**MAY, 2023**

DELHI TECHNOLOGICAL UNIVERSITY

(Formerly Delhi College of Engineering)

Bawana Road, Delhi – 110042

**CANDIDATE’S DECLARATION**

I, SHASHWAT VASHISTHA, 2K21/STE/19, of M.Tech (Structural Engineering), hereby declare that the project Dissertation titled “CFD analysis for wind flow characteristics of various facades in an H-shaped tall building using ANSYS CFX” which is submitted by me to the Department of Civil Engineering, Delhi Technological University, Delhi in partial fulfilment of the requirement for the award of the degree of Master of Technology, is original and not copied from any source without proper citation. This work has not previously formed the basis for the award of any Degree, Diploma Associateship, Fellowship, or other similar title or recognition.

Place: Delhi

**SHASHWAT VASHISTHA**

Date:

DELHI TECHNOLOGICAL UNIVERSITY

(Formerly Delhi College of Engineering)

Bawana Road, Delhi – 110042

**CERTIFICATE**

I hereby certify that the Project Dissertation titled “CFD analysis for wind flow characteristics of various facades in an H-shaped tall building using ANSYS CFX” which is submitted by SHASHWAT VASHISTHA, 2K21/STE/19, Department of Civil Engineering, Delhi Technological University, Delhi in partial fulfillment of the requirement for the award of the degree of Master of Technology, is a record of the project work carried out by the student under my supervision. To the best of my knowledge, this work has not been submitted in part or full for any Degree or Diploma to this University or elsewhere.

Place: Delhi

**DR. RITU RAJ AHIRWAR**

Date:

**SUPERVISOR**

## **ABSTRACT**

Tall buildings have been an intriguing concept to look at with a vast scope for improvement in the design capabilities against lateral wind and earthquake loads, and their behavior due to the same. The major load-resisting capacity to be analyzed and strengthened against high-rise structures is the Lateral Wind Load. This study investigates the accuracy of computational fluid dynamics (CFD) simulations for predicting the wind characteristics around a high-rise building of various façade. A 60m high H-shaped building with a span area of around 200 square meters scaled down to a ratio 1:100, modeled for isolated and interference conditions using ANSYS CFX and subjected to lateral wind loading at different incidents angles (0 to 360 degrees) between wind and windward face in Virtual Wind Tunnel. The results show the wind pressure experienced by the building is maximum at an incidence angle of 30° and negative wind pressure i.e. suction phenomenon is maximum at an incidence angle of 60°; Variation of the wind pressure and average wind pressure using pressure contours and respective Coefficient of wind pressure due to lateral wind load on each façade is obtained using the Power Law Equation, are then calculated and mean variation along the faces Face-Average  $C_p$  has been calculated, plotted and discussed to a great extent.

## ACKNOWLEDGEMENT

I would like to offer my heartfelt appreciation to everyone who helped me finish this academic project. This initiative would not have been feasible without their assistance and support.

First and foremost, I would want to thank **Dr. Ritu Raj Ahirwar** (Assistant Professor, Delhi Technological University), my academic project supervisor, for leading me through the project and giving me vital insights and criticism. I appreciate the time and work he has put into me.

I would like to thank **Prof. V K Minocha** (Head of the Department, Delhi Technological University), **Dr. Shilpa Pal** (Associate Professor, Coordinator) and other teachers for motivating and inspiring me throughout this journey, and for their brilliant comments and suggestions.

I also want to thank my family and friends for their constant support and encouragement during this effort. Their faith in me has been both motivating and inspiring.

Finally, I'd want to thank God for allowing me to go through all of this. Day by day, I've felt your leadership. You are the one who allowed me to complete my degree. I will continue to put my faith in you for my future.

SHASHWAT VASHISTHA

## CONTENTS

<b>Candidate's Declaration</b>	<b>i</b>
<b>Certificate</b>	<b>ii</b>
<b>Abstract</b>	<b>iii</b>
<b>Acknowledgment</b>	<b>iv</b>
<b>Content</b>	<b>v</b>
<b>List of Tables</b>	<b>viii</b>
<b>List of Figures</b>	<b>ix</b>
<b>List of Symbols and Abbreviations</b>	<b>xi</b>
<b>CHAPTER 1 INTRODUCTION</b>	<b>1</b>
1.1. Overview	1
1.2. High-rise building	1
1.3. Loading conditions for high-rise structures	2
1.3.1. Wind load	3
1.4. Finite Element Method and Ansys CFX	5
1.4.1. Ansys CFX Workbench	5
1.4.2. Computational Fluid Dynamics	6
1.5. Objectives of the study	7
<b>CHAPTER 2 LITERATURE REVIEW</b>	<b>8</b>
2.1. Overview	8
<b>CHAPTER 3 METHODOLOGY</b>	<b>12</b>
3.1. General	12
3.2. Wind Load Analysis	12

3.2.1. Characteristics of wind	13
3.2.1.1. Boundary Layer Concept	13
3.2.1.2. Wind Profiles	14
3.2.2. Mathematical Equations and Modeling	15
3.2.3. Concept of Power Law	17
3.2.4. Virtual Wind Tunnel in ANSYS	17
3.3. Finite Element Analysis	19
3.4. CFD Simulation using Ansys CFX	20
3.4.1. Validation using IS: 875 Part 3 (2015)	20
3.4.2. Isolated Building Study	20
3.4.3. Interference Study	21
3.5. Modeling And Simulations	22
3.5.1. Geometry	23
3.5.1.1. Validation Model	23
3.5.1.2. Virtual Wind Tunnel (Domain)	23
3.5.1.3. Isolated Model	25
3.5.1.4. Interference Model	26
3.5.2. Meshing	28
3.5.2.1. Model Sizing Meshing	28
3.5.2.2. Domain Sizing Meshing	28
3.5.2.3. Inflation Meshing	29
3.5.2.4. Automatic Default Meshing	29
3.5.3. Setup and Boundary Conditions	30
3.5.3.1. Boundary condition	30
3.5.3.1.1. INLET of Domain	30
3.5.3.1.2. OUTLET of Domain	30

3.5.3.1.3. SIDE WALLS of Domain	30
3.5.3.1.4. GROUND of Domain	31
3.5.3.2. Setup for Simulation	32
<b>CHAPTER 4 RESULTS AND DISCUSSIONS</b>	<b>34</b>
4.1. General	34
4.2. Simulation Results	34
4.2.1. Line method	34
4.2.2. Pressure Contours	35
4.2.3. Velocity Streamlines	36
4.2.4. Coefficient of Pressure	37
4.3. Validation Results	37
4.4. Isolated Study	38
4.4.1. Effect of Wind incident angle	42
4.5. Interference Study	46
4.5.1. Effect of Wind incidence angles	48
<b>CHAPTER 5 CONCLUSIONS</b>	<b>51</b>
<b>REFERENCES</b>	<b>53</b>
<b>LIST OF PUBLICATIONS</b>	<b>57</b>



## LIST OF TABLES

Table 1.1	Loads Combinations As Per Is: 875 (Part 5)	3
Table 3.1	Three Interference Conditions Of H-Shaped Building	27
Table 3.2	Input Values Used In Setup	32
Table 4.1	Validation Results Of Square Model	38
Table 4.2	Average Pressure At Different Wind Incidence Angles	44
Table 4.3	Maximum Positive Wind Pressure (Pa) At Different Angles In Interference	49
Table 4.4	Maximum Negative Wind Pressure (Pa) At Different Angles In Interference	50

## LIST OF FIGURES

Fig 1.1	(a) Effect of Wind load on tall structure; (b) Variation of wind pressure with height of building.	4
Fig 3.1	A typical Wind Velocity vs. Time variation	12
Fig. 3.2	Influence of Terrain and Topography on wind	13
Fig. 3.3	Boundary layer flow at different types of terrain	14
Fig. 3.4	Variation of Wind Velocity vs. Height	15
Fig. 3.5	Dimensions of wind tunnel	18
Fig. 3.6	Virtual Wind Tunnel	18
Fig. 3.7	2D Elements for Finite Element Analysis	19
Fig. 3.8	3D Elements (a) Tetrahedron; (b) Rectangular (Brick); (c) Arbitrary Hexahedron; (d) 3D Quadratic	19
Fig. 3.9	(a) Plan & (b) Elevation of Standard Square model for Validation	20
Fig. 3.10	Wind Flow around an Isolated building	21
Fig. 3.11	Interference effect of Wind	22
Fig. 3.12	Flow diagram of Ansys CFX	22
Fig. 3.13	(a) Plan, (b) Elevation, & (c) Model of Square Validation model	23
Fig. 3.14	Dimensions of wind tunnel in side elevation	24
Fig. 3.15	Dimension of the Domain in 3D view	24
Fig. 3.16	Wind Tunnel Domain in Ansys	25
Fig. 3.17	Plan and Isometric view of the H-shaped building	25
Fig. 3.18	Isolated H-shaped Building model	26
Fig. 3.19	Model after meshing	28
Fig. 3.20	Inflation meshing	29
Fig. 3.21	Model after Boundary condition are applied	31
Fig. 3.22	Equation setup in Ansys CFX	32
Fig. 4.1	Pressure lines in H-shaped building	35

Fig. 4.2	Typical pressure contour in ANSYS CFX	36
Fig. 4.3	Typical pressure contour in ANSYS CFX	37
Fig. 4.4	Plan and Isometric view of the H-shaped building	39
Fig. 4.5	(a) H-shaped building model and (b) Domain in Ansys	39
Fig. 4.6	Pressure Contour of the Isolated H-shaped model	40
Fig. 4.7	Variation of Pressure with the increasing height of the building	40
Fig. 4.8	Velocity Streamline for Isolated H-shaped building	41
Fig. 4.9	Variation $C_p$ along the height of the building	41
Fig. 4.10	Pressure contour and Velocity streamlines at different angles of incidence	43
Fig. 4.11	Graphical comparison of max wind pressure at different angles	44
Fig. 4.12	(a) $C_p$ (b) Wind pressure at different wind incident angles along the height of the model	45
Fig. 4.13	Interference between two H-shaped buildings	47
Fig. 4.14	Pressure contours for interference conditions in H-shaped buildings	47
Fig. 4.15	Velocity Streamlines for interference conditions oh H-shaped buildings	48
Fig. 4.16	Graphical representation of Max Wind pressure at different angles in Interference	49
Fig. 4.17	Graphical representation of Max Wind pressure at different angles in Interference	50

## LIST OF SYMBOLS AND ABBREVIATIONS

$\alpha$	Power Law constant
$\rho$	Density of air
$U_{ref}$	Reference Velocity of wind
$Z_{ref}$	Reference height at which $U_{ref}$ is measured
DL	Dead Load
LL	Live Load
IL	Imposed Load
EL	Earthquake Load
WL	Wind Load
TL	Temperature Load
IB	Interfering Building
PB	Principal Building
CFD	Computational Fluid Dynamics
$C_p$	Coefficient of Wind Pressure
FE	Finite Element
LES	Large Eddy Simulation
V	Wind Velocity
FEA	Finite Element Analysis

# **CHAPTER 1**

## **INTRODUCTION**

### **1.1. OVERVIEW**

The most prevalent type of buildings in urban development is multi-story and high-rise structures. A high-rise building is subject to lateral wind load, which is the principal horizontal load. It is essential to provide a load-bearing system that can handle the force of wind for guaranteeing the steadiness and solace of somebody on the top or base floors. The windward pressure and the eddy flows from the leeward side of a high-rise building both grow as new development's height rises. In addition to static wind loads that rise with building height, aero-elastic dynamic vibrations also occur, the value of which frequently predominates. The distribution of wind pressure along a building or structure's height, as well as the impact of air flows on buildings nearby, and other factors make the impact of wind load on high-rise buildings quite interesting.

### **1.2. HIGH-RISE BUILDING**

According to national building code of India, In India, a building structure can be considered to be High-rise when the height of that particular building is greater than or equal to 15m above ground level.

For structural and geotechnical engineers, high-rise structures present unique design issues, especially if they are situated in regions that are prone to earthquakes or if the soils beneath them contain geotechnical risk factors such as high compressibility or bay mud.

Numerous structural issues, including stiffness, lateral displacement, and lateral load impact, are evident in high-rise buildings. In general, wind and seismic load impacts are dominant for high-rise structures. Therefore, it is imperative for a high-rise construction to analyze these loads and how they affect the structure. Super-tall structures have been built thanks to innovative scientific and commercial development, advancements in construction methods, the use of strong materials, and inventive architectural design.

The shape of the building faces also affects the behavior of the building in response towards the unpredictable wind loads which are the major acting forces on the high-rise building.

The relationship between the magnitude of the wind load and its behavior w.r.t. the particular high-rise also depends on the location of the building and the respective average wind velocity in that particular location.

In this study, a 60m tall H-Shaped building is chosen to study the wind flow characteristics over the different faces of the building in isolated and an interference study between two H-shaped building modeled to be situated in a near coastal region in India where standard wind velocity is 10m/s at the height 1m from ground and increases with the increasing height of the building.

### **1.3. LOADING CONDITIONS FOR HIGH-RISE STRUCTURES**

The major external load experienced by any structure for which it is to be designed is either earthquake load or wind load. For high-rise structures the major external load that affects the structural response of the building is lateral wind load.

Over a long period of time, they have caused roughly the same amount of damage, although large, destructive earthquakes occur less frequently than severe wind storms.

Although seismic loading and wind loading are the two primary environmental loads on structures, but only one of them will be taken into consideration while

designing the building structure. Along with the various loads such as dead load (DL), live load (LL), and other loads acting on the building there will be either only earthquake load (EL) or only wind load (WL) that will be considered for the designing of the building.

Indian standard code **IS: 875 (Part 5)**, Code of Practice for Design Loads (Other than Earthquake) for Building and Structures- Part 5 Special Loads and Combination, provides guidelines for the various load combinations that can act on any building as shown in Table 1.1.

**Table 1.1 Loads combinations as per IS: 875 (Part 5)**

<ul style="list-style-type: none"> <li>a) DL</li> <li>b) DL + LL</li> <li>c) DL + WL</li> <li>d) DL + EL</li> <li>e) DL + TL</li> <li>f) DL + IL + WL</li> <li>g) DL + IL + EL</li> <li>h) DL + IL + TL</li> <li>i) DL + WL + TL</li> <li>j) DL + EL + TL</li> <li>k) DL + IL + WL + TL</li> <li>l) DL + IL + EL + TL</li> </ul>	<p>Where,</p> <p>DL = Dead Load            LL = Live Load            WL = Wind Load            EL = Earthquake Load            IL = Imposed Load            TL = Temperature Loads</p>
--	--

This study deals with the study of the wind loads and its characteristics on a high-rise structure using CFD simulations by creating a virtual wind tunnel in ANSYS CFX Workbench 2022 R2 Student version.

### **1.3.1. Wind load**

The wind has two sides. The first, which is good, is that its energy can be used to make power, sail boats, and cool things down on hot days. The other - a parasitic one - is that it stacks every item that comes in its manner. Since the load must be supported by a structure that meets the specified safety standards, the latter aspect is the one that engineers are concerned with. All civil and industrial structures over the ground must be intended to resist wind loads.

IS: 875, Part- 3 Wind Loads[28], specifies the static and dynamic effects of wind forces that must be taken into account when designing structures, buildings, and their components.

Appraisal of wind loads and reaction expectations are urgent in the plan of various structures and designs because of the arbitrariness of wind speeds across existence. However, the vast majority of structures encountered in practice do not exhibit wind-induced oscillations, so dynamic wind effects testing is typically unnecessary. Static wind analysis has proven to be useful in estimating loads for such typical, tall, and short structures.

Fig. 1.1 shows the effect of wind on a tall building, where Fig. 1.1 (a) shows the effect of wind load on tall structure in terms of deflection shape, shear force and bending moment diagrams, whereas, Fig. 1.1 (b) shows the variation of wind pressure with height of the building.

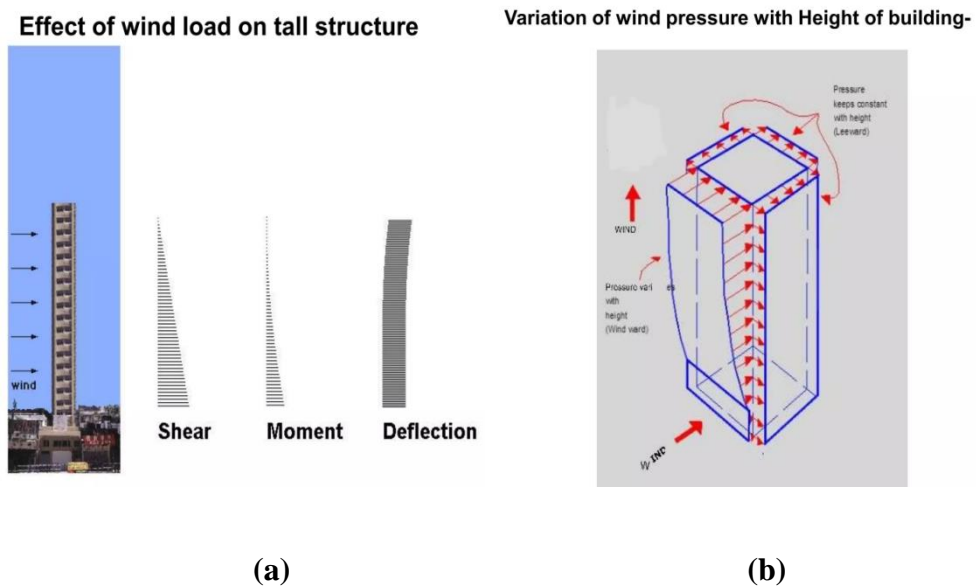


**Fig. 1.1 (a) Effect of Wind load on tall structure; (b) Variation of wind pressure with height of building.**



## **1.4. FINITE ELEMENT METHOD AND ANSYS CFX**

The finite element analysis (FEA) is a numerical technique. The issues' all's intricacies, including changing shape, limit conditions, and loads, are protected in this methodology, yet estimated arrangements are gotten. It is receiving a lot of attention in engineering due to its versatility and variety as an analysis tool. Since a PC is vital for the strategy's execution, fast headways in PC equipment innovation and cost decreases have helped it. Industrially accessible limited component investigation bundles incorporate various notable brands. STAAD-Star, GT-STRUDEL, NASTRAN, NISA, and ANSYS are among the well-known bundles. The analysis of numerous intricate structures is made possible by these packages.

The first application of the method known as finite element analysis was to conduct stress tests on airplane plans. The structural analysis matrix method served as the foundation for it in the beginning. In addition to solid mechanics, this method is currently used to investigate fluid flow, heat transfer, electric and magnetic fields, and a wide range of other phenomena. Civil engineers use this method a lot to look at beams, space frames, plates, shells, folded plates, foundations, rock mechanics issues, and fluid seepage analysis through porous media. Static and dynamic problems can be solved with finite element analysis. Boats, airplanes, spacecraft, electric engines, and intensity motors are all extensively studied and planned using this method.

### **1.4.1. ANSYS CFX Workbench**

Engineering simulation software for use throughout the product life cycle is developed and offered by Ansys. Ansys Mechanical limited component examination software is used to analyze the strength, durability, versatility, temperature transmission, electromagnetism, liquid stream, and other characteristics of designs, hardware, or machine parts by imitating PC models. Without the need to build test items or complete accident tests, Ansys is used to learn how an item will perform under different particulars. For instance, Ansys

software might simulate how a bridge will hold up to years of traffic, how to reduce waste when processing salmon in a cannery, or how to design a slide that uses less material without compromising safety.

The Ansys Workbench system, one of the company's main products, is used for the majority of Ansys simulations. Most of the time, people who use Ansys break down larger structures into smaller parts that are each modeled and tested separately. A customer might begin by describing an item's elements, then add weight, tension, temperature, and other actual properties. Finally, the Ansys software reconstructs and dissects long-term effects like development, exhaustion, cracks, liquid stream, temperature dispersion, electromagnetic productivity, and others.

#### **1.4.2. Computational Fluid Dynamics**

Computational Liquid Elements (CFD) is a part of fluid mechanics that uses numerical assessment and data plans to take apart and tackle gives that incorporate fluid streams. The computations are necessary to reproduce the free stream of the liquid and the interaction of the liquid (fluids and gases) with surfaces with limit conditions are carried out using computers. High-speed supercomputers are frequently required to solve the largest and most complex problems, making better solutions possible.

In this study, to perform the CFD study of wind around a tall building, ANSYS CFX software package is being used which is provided by Ansys Workbench.

## **1.5. OBJECTIVES OF THE STUDY**

In this study, a 60-meter-tall H-shaped building is chosen to investigate the characteristics of wind flow across the building's various faces in isolation and in interference between two H-shaped buildings that are modeled to be in a near-coastal region in India. The standard wind velocity is 10 meters per second at a height of one meter above the ground and increases with building height using CFD simulations in ANSYS CFX Workbench 2022 R2 Student version.

**Objectives** of the study are as follows –

- 1.** CFD Analysis for Wind Flow Characteristics of Various Facades in an H- SHAPED High-Rise Building Using ANSYS CFX.
- 2.** To study the INTERFERENCE Effects between TWO H-SHAPED High-rise buildings of different shapes under wind load using CFD simulations.

## CHAPTER 2

### LITERATURE REVIEW

#### 2.1. OVERVIEW

A literature review is a comprehensive summary of previous research on a topic. The books, academic articles, and other sources relevant to a given field of study are examined in the literature review. The recognition of previous analyses in the literature review provides the pursuer with assurance that your work has been carefully considered.

The reader will learn about the concepts, knowledge, and strengths and weaknesses that have been developed on a subject. The literature review should be characterized by a directing idea (e.g. your argumentative thesis, the problem or issue you're addressing or your research objective). It is not merely a collection of summaries or a descriptive list of the available resources.

This chapter consists of the literature review of numerous publications done to understand the concept of the wind loading and the CFD analysis done to study the characteristics of the wind and the response of the structures when are exposed to it.

**Ali Khalilzadeh, et al. (2019)** published a paper in which the study centers around validation of CFD modeling of Wind Driven Rain (WDR) on a mid-rise building. A six-story building's wind flow around and WDR deposition are examined in relation to turbulence modeling. Wind-tunnel measurements were completed to approve. Wind stream reproductions. WDR simulation results are

contrasted with full-scale field estimations. . It is shown that stand-alone structure answer for such recreations is conceivable and, at times, suggested.

**Yong Wang, et al. (2022)** gave a study to verify the accuracy of large-eddy simulation (LES) of wind pressures and loads on high-rise buildings at various angles of attack. The study is based on an approaching flow simulation framework with synthesized inflow turbulence. By contrasting the reproduction results from different degrees of lattice refinement to the trial information, its precision is illustrated. Wind pressure skewness and kurtosis predictions, which are crucial for predicting peak pressures, can be improved with octree mesh refinement, as shown. The probability distribution of peak pressures from short simulation sample durations is improved using a moment-based Hermite model.

**Chaorong Zheng, et al. (2018)** did their work in which Characteristics of wind induced responses of tall building under combined aerodynamic control are analyzed including cross-sectional shape optimization (i.e. square, corner recessed or chamfered square, Y- shaped etc.).

**Bin Yang, et al. (2022)** presented paper giving a Kalman channel based breeze load reversal calculation for elevated structures, Speed increase reactions got from few estimated stories can be utilized in this way to deal with distinguish the breeze load on a really tall building structure. Based on the results of a dynamic analysis of the finite element (FE) model and the wind load of the numerical wind tunnel test, the Kalman filter method was used to invert the wind load. The decrease of the modular space, the effect of estimation commotion, the effect of a wrong assessment of the underlying worth, and the effect of presenting the mean breeze load are only a couple of the vital parts of this reversal calculation that are examined in this paper.

**J. Shanmugasundaram, et al. (2000)** gave a review report based on a case study about types of damages that occur in different types of structures based on Indian cyclonic conditions. Mitigation measures for cyclone-resistant design and construction are provided by detailed study of the disaster surveys conducted by SERC, Madras, on damage caused to several buildings and structures.

**Ark Rikhaiyar, et al. (2022)** presented a paper showing a comparative study between various cross-sections of a high-rise building under wind-induced effects on the building and finding about optimum shape under given circumstances. It was discovered from pressure contours that the face's shape and size are unaffected by the pressure distribution. Additionally, the pressure distribution on the windward face for each model was smaller than that on the leeward face. The leeward face and horizontal appearances had comparative strain dissemination. At the models' periphery, a few alterations in pressure distribution were also observed.

**Devesh Kasana et al. (2022)** gave a review that spotlights on deciding what wind means for high-rise structures of seven distinct customary shapes that have a similar base region and height. The wind pressure on each of the building model's faces is calculated using the ANSYS CFX for Computational Fluid Dynamics studies.

**Sumit Verma et al. (2022)** made an endeavor to approve a CFD model by differentiating the tensions created by cyclone like vortices on a structure model with exploratory estimations taken at Texas Tech College's (TTU) twister test system. The comparison demonstrates that the pressure coefficients from the TTU experimental datasets and the CFD model are in good agreement. Additionally, pressure coefficients on the structure caused by cyclone-like vortex are investigated in relation to the effects of building size and stream design. The vortex with a single celled structure produces the most unfavorable loading conditions for the building model, and it has been observed that the building's pressures can vary by up to 100% when different building sizes are taken into account.

**Fangwei Hou et al. (2020)** gave a review paper in light of the past examinations on wind reaction of tall structures alongside the information on the mechanism and identification techniques. Through comparison of previous studies, the extensive literature reviewed here can assist in gaining a deeper comprehension of the effects of wind-induced loads on tall buildings and provide intuitive insights.

**Anoop Kodakkal et al. (2022)**, in his study proposed a novel risk-averse shape optimization strategy for tall building design that takes into account site-specific uncertainties. Optimizing at a risk-averse level reduces the likelihood of high-loading scenarios. He used adaptive sampling to converge the design algorithm and accelerate, which is simple to implement and useful for computer-intensive simulations with more samples. The risk-averse design strategy's efficacy in computational wind engineering was then demonstrated.

## CHAPTER 3

### METHODOLOGY

#### 3.1. GENERAL

This chapter consists of the study's approach to research of the characteristics of the wind w.r.t. a tall building. Various characteristics profiles of wind of wind are discussed. Finite Element Method and its applications are discussed. CFD modeling and simulations using ANSYS CFX are shown for, first, validation of the modeling and, second, modeling and simulation of the selected tall building.

#### 3.2. WIND LOAD ANALYSIS

Wind is a dynamic phenomenon that changes at random, and a trace of wind velocity against time will typically look like the fig. 3.1. The "gustiness" caused by the wind velocity  $V$  can be thought of as a mean plus fluctuating component.

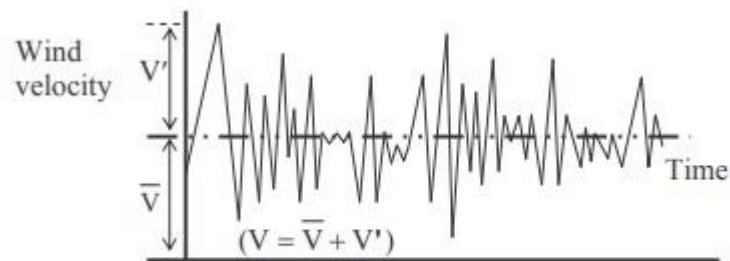


**Fig. 3.1 A typical Wind Velocity vs. Time variation**



### 3.2.1. Characteristics of wind

Wind characteristics include the various profiles of the wind velocity, boundary layer phenomenon due to the earth's surface friction. Fig. 3.2 shows a general characteristic profile of wind at different terrain.

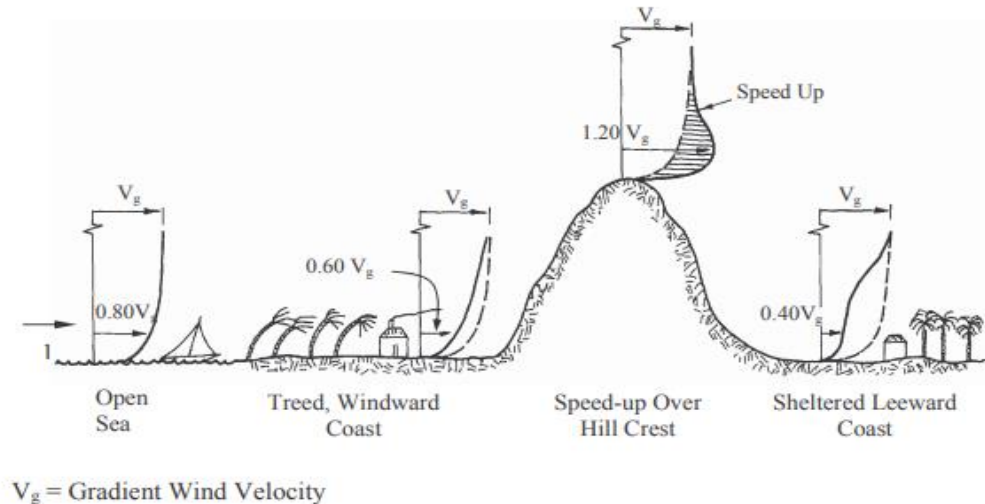


**Fig. 3.2 Influence of Terrain and Topography on wind**

#### 3.2.1.1. Boundary Layer Concept

The region of wind flow that is affected by friction at the earth's surface, which can extend up to one kilometer, is referred to as the "boundary layer." As the wind speed decreases closer to the surface of the earth, the Coriolis forces gradually decrease in magnitude. This makes the geostrophic balance be upset, and the mean wind vector abandons being lined up with the isobars to having a part towards low tension, as the level over the ground decreases. As a result, height and magnitude may cause a slight shift in the mean wind speed.

The primary properties of airflow with a fully formed "boundary-layer" is:

- Increasing height causes the average wind speed to rise.

- At all height, the wind speed has gusty and turbulent nature.
- The broad range of frequencies in the gusts in the air flow.
- There is some similitude in the examples of gusts at all heights, particularly for the more leisurely evolving gusts, or lower frequencies.

Fig. 3.3 shows the change in the boundary layer with topography.

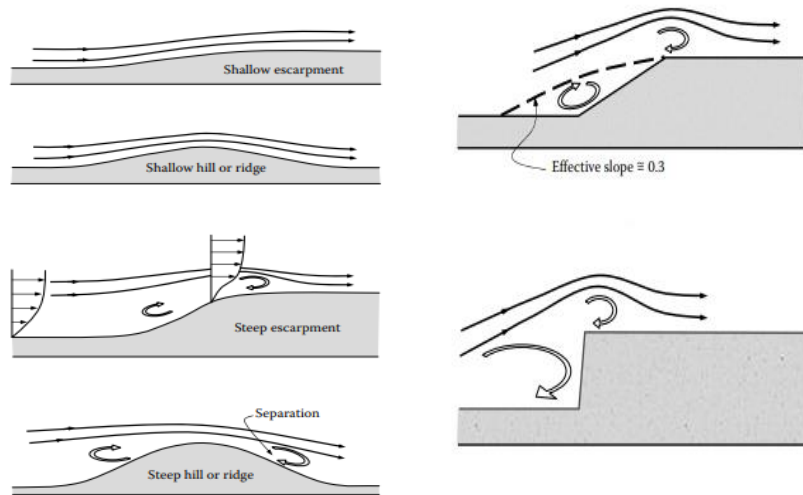


**Fig. 3.3 Boundary layer flow at different types of terrain**

### 3.2.1.2. *Wind Profiles*

Tall and thin designs are versatile and show a unique wind response. Because of the partition of the stream and the innate disturbance of the wind, as well as the turbulence produced by the actual construction, tall designs vibrate in the wind. The result is a mean and fluctuating response from the wind. Additionally, because the dynamic forces act not only in the direction of wind flow but also in a direction that is nearly perpendicular to the flow (lift forces), tall structures exhibit an across-wind response.

Fig. 3.4 shows the mean variation of the wind with the increase in the height. Wind velocity is less near the ground due to the friction of the earth surface and increases with the height.

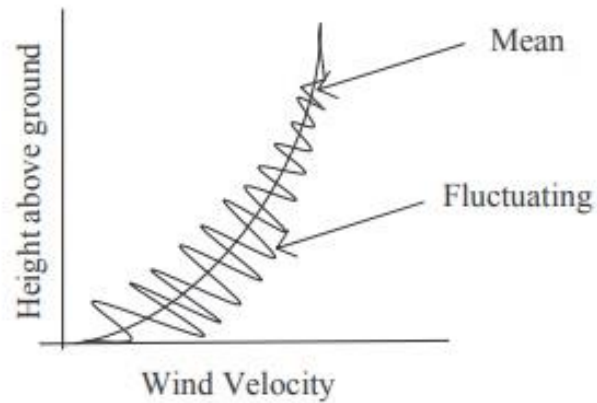


**Fig. 3.4 Variation of Wind Velocity vs. Height**

### 3.2.2. Mathematical Equations and Modeling

Computational Fluid Dynamics can be understood by the help of some mathematical equations that governs the fluid flow. Some of the equations of Computational Fluid Dynamics are stated below.

The CFD software package of Ansys gives numerous turbulence models. In contrast to wind tunnel experiments, however, only a proper turbulence model flow profile produces accurate results. The exactness fundamentally relies on the computational grids and discretization technique consolidated. Numerical predictions are confirmed by their correlation with the consequences of an air stream extraordinary examination. The standard k- $\epsilon$  disturbance model has been creating the quickest and precise outcomes aside from non-isotropic k- $\epsilon$  choppiness reproductions.

- *Continuity equation Non-conservation form*

$$\frac{D\rho}{Dt} + \rho \nabla \cdot \vec{V} = 0 \quad (3.1)$$

- *Continuity equation conservation form*

$$\frac{dy}{dx} + \nabla \cdot (\rho \vec{V}) = 0 \quad (3.2)$$

- *Navier-Stokes equation is as follows:*

Newton's second law of motion serves as the foundation for this momentum equation.

$$\frac{\partial(\rho u_i)}{\partial t} = -\frac{\partial(\rho u_i u_j)}{\partial x_j} - \frac{\partial P}{\partial x_j} + \frac{\partial}{\partial x_j} \left[ \mu \left( \frac{\partial u_i}{\partial x_j} + \frac{\partial u_j}{\partial x_i} \right) \right] + F \quad (3.3)$$

Models from several fields are used to underpin computational fluid dynamics. K-model is employed in this investigation.

- *Standard k-ε model*

The k-ε model is used in computational fluid dynamics to determine flow characteristics under a variety of flow conditions. Our investigation only takes into account the steady flow condition. Numerous studies utilized this strategy, which consistently yielded favorable outcomes. When previous results are taken into account, this model has demonstrated itself to be reliable and stable. When compared to wind tunnel investigations, simulations are quite affordable. Two equations underpin this model, which are

- Turbulent kinetic energy equation,

$$\frac{\partial y}{\partial x} + \frac{\partial y}{\partial x} = \frac{\partial y}{\partial x} + 2\mu_t E_{ij} E_{ij} - \rho \varepsilon \quad (3.4)$$

- Dissipation equation,

$$\frac{\partial(\rho \varepsilon)}{\partial t} + \frac{\partial(\rho \varepsilon u_i)}{\partial x_i} = \frac{\partial}{\partial x_j} \left[ \frac{\mu_\varepsilon}{\sigma_\varepsilon} \frac{\partial \varepsilon}{\partial x_j} \right] + C_{1\varepsilon} \frac{\varepsilon}{k} 2\mu_t E_{ij} E_{ij} - C_{1\varepsilon} \rho \frac{\varepsilon^2}{k} \quad (3.5)$$

Where,  
 $u_i$  is velocity component in their respective directions.  
 $E_{ij}$  is the rate of deformation or strain rate  
 $C_{1\varepsilon}, C_{2\varepsilon}$  are constants.

### 3.2.3. Concept of Power Law

Understanding the characteristics of wind is extremely challenging due to its inherent complexity. Wind patterns are impacted by different variables, including the environment, topography, and land advancement. However, the fundamental idea that ground-level friction causes wind velocity to be low applies to all types of wind. As the wind rises from the ground, its speed increases.

In context of this idea, the following empirical velocity distribution formula is provided.

$$U = U_{ref} \left( \frac{Z}{Z_{ref}} \right)^\alpha \quad (3.6)$$

Where,

- $U_{ref}$  is reference wind velocity (m/s),
- $U_{ref}$  at the top of the building is 10 m/s
- $Z_{ref}$  is reference height above ground; generally taken as 1 m ,
- $U$  is wind velocity at  $Z$  height above ground level,
- $\alpha$  is power law constant which depends on type of terrain, ground roughness, generally taken as 0.143.

### 3.2.4. Virtual Wind Tunnel in ANSYS

In order to do the study of wind characteristics around a tall building, it is required to analyze the building in the wind tunnel. But in real life conditions, if the building to be analyzed is of the height  $H$ , then wind should be of the size  $6H*20H*6H$ , as shown in the fig. 3.5.

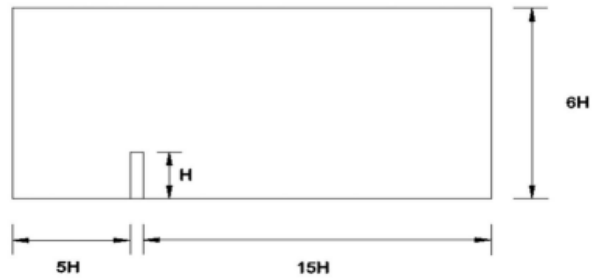


**Fig. 3.5 Dimensions of wind tunnel**

Since it is practically impossible to make wind tunnel for the real life structures, we first make miniature models of the structures and then we test it in the wind tunnel.

But sometimes testing of the structure in the wind tunnel is also could not be done mostly in absence of the experimental apparatus. Hence software simulations provide solutions that we can access and perform anywhere as per our convenience.

In this study ANSYS CFX package provided by Ansys Workbench 2022 R2 is used to model the building and simulate in the Virtual Wind Tunnel to analyze the wind flow characteristics on a tall building. Fig. 3.6 shows scale down model of the building inside the Virtual Wind Tunnel made using Ansys CFX.

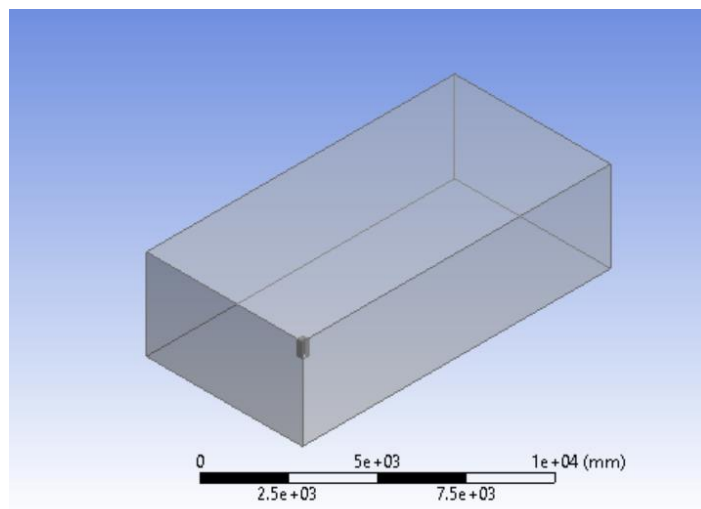


**Fig. 3.6 Virtual Wind Tunnel**

### 3.3. FINITE ELEMENT ANALYSIS

Finite Element Analysis is the solution technique a large problem by creating divisions of small elements and then solving each element individually and then by combining the results to get the whole solution.

In this method, nodes and elements are chosen to divide the whole structure surface into small elements to solve the structure.

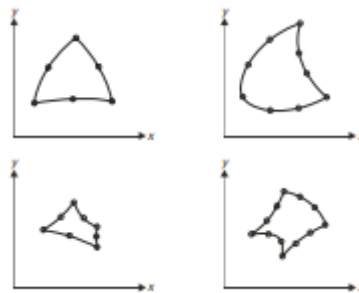


**Fig. 3.7 2D Elements for Finite Element Analysis**

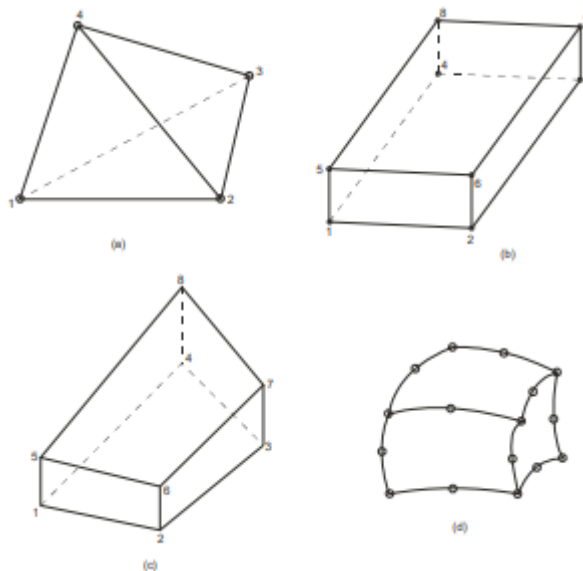


**Fig. 3.8 3D Elements (a) Tetrahedron; (b) Rectangular (Brick); (c) Arbitrary Hexahedron; (d) 3D Quadratic**

Fig. 3.7 and 3.8 shows some examples of the basic elements to be chosen for the Finite Element Modeling of any structure.

### 3.4. CFD SIMULATION USING ANSYS CFX

#### 3.4.1. Validation using IS: 875 Part 3 (2015)

The ANSYS CFX package's validity is examined prior to beginning the building's numerical analysis. Consequently, a square model formed working of cross-section  $200 \text{ mm} \times 200 \text{ mm}$  as displayed in fig. 3.9.

The results are used to find out the  $C_p$  i.e. coefficient of wind pressure on the faces of square model and are then compared with standard results given in various design codes.

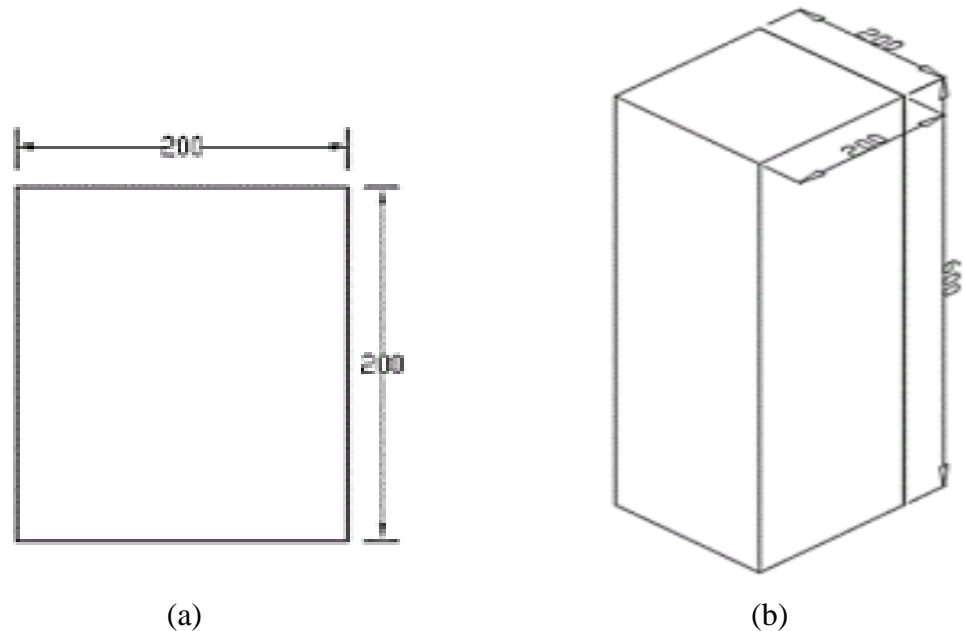


**Fig. 3.9 (a) Plan & (b) Elevation of Standard Square model for Validation**

#### 3.4.2. Isolated Building Study

Tall and slender structures are adaptable and show a dynamic wind response. Because of the separation of the flow and the inherent turbulence of the wind, alongside the turbulence created by the building itself, tall structures vibrate in the wind. As a result, the wind causes a mean and fluctuating response. In addition, tall



structures exhibit an across-wind response because the dynamic forces work toward wind stream as well as toward a path that is perpendicular to the stream (lift forces).

Fig. 3.10 shows a typical wind behavior around an isolated building when subjected to the wind load.

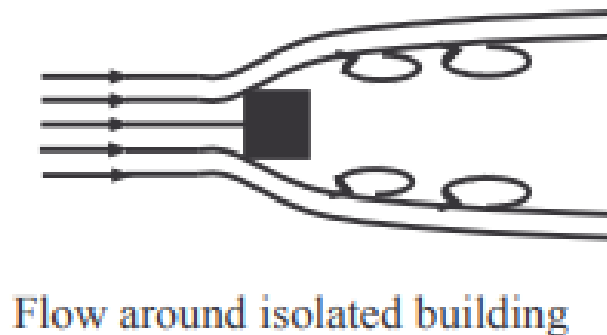


**Fig. 3.10 Wind Flow around an Isolated building**

### **3.4.3. Interference Study**

A body or a design, like a structure, chimney or transmission towers, when placed in a movement of air will experience pressure and forces. The "isolated" upsides of pressures and forces change when various comparable or divergent bodies are put downstream or upstream of a design. This is named as the Interference Effect.

Whether the bodies in question are rigid or flexible, interference will occur. Despite the fact that it occurs frequently in practice, the phenomenon of interference is difficult to quantify due to the wide range of circumstances involved.

However, systematic wind tunnel studies can provide some direction. Fig. 3.11 shows a typical interference effect between two bodies.

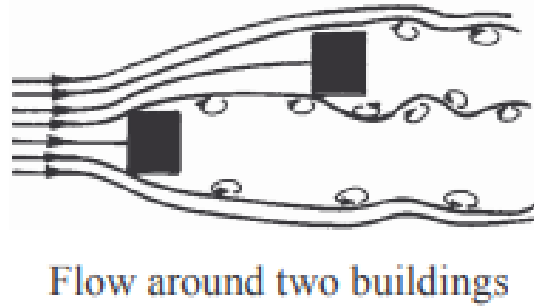


**Fig. 3.11 Interference effect of Wind**

### 3.5. MODELING AND SIMULATIONS

ANSYS CFX by Ansys Workbench 2022R2 software package has been used to perform this study. A general flow diagram of the working of the project in Ansys has been shown in the fig. 3.12.

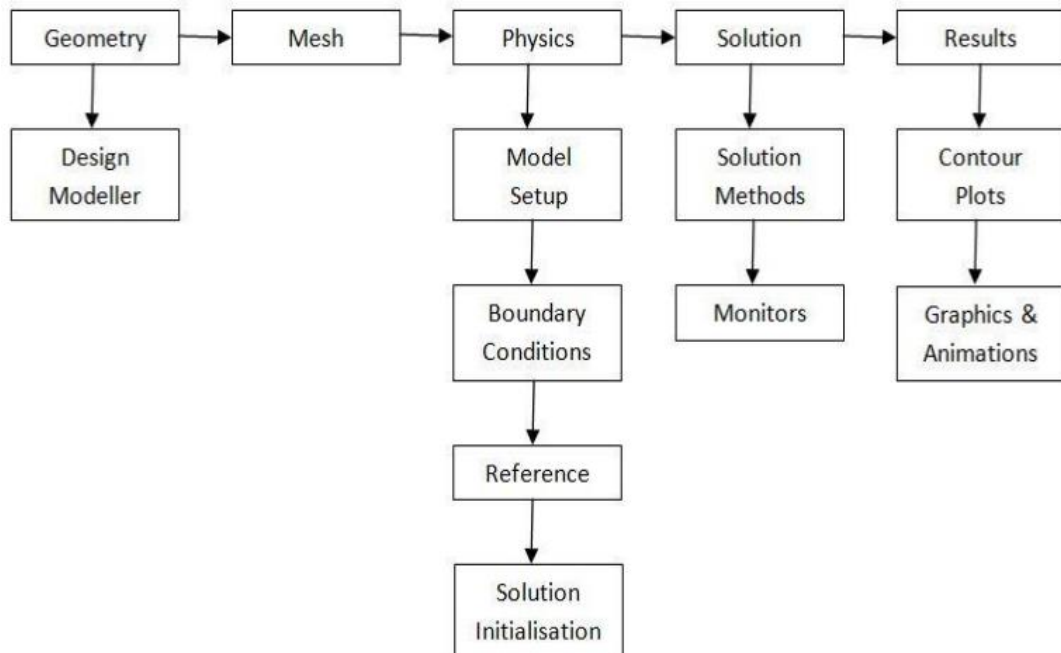


**Fig. 3.12 Flow diagram of Ansys CFX**

### 3.5.1. Geometry

All the required geometries of the study are being made in the ANSYS CFX design modeler feature with the scale of 1: 100 from any actual building body.

Various numbers of models are made for the study.

#### 3.5.1.1. Validation Model

To validate study, a standard Square shaped building model or dimensions 200mm\*200mm\*600mm is modeled to validate for the wind flow properties in accordance with the IS: 875 Part 3, IS code for Wind Loads on structures.

Fig. 3.13 shows the plan elevation and model of the Square building.

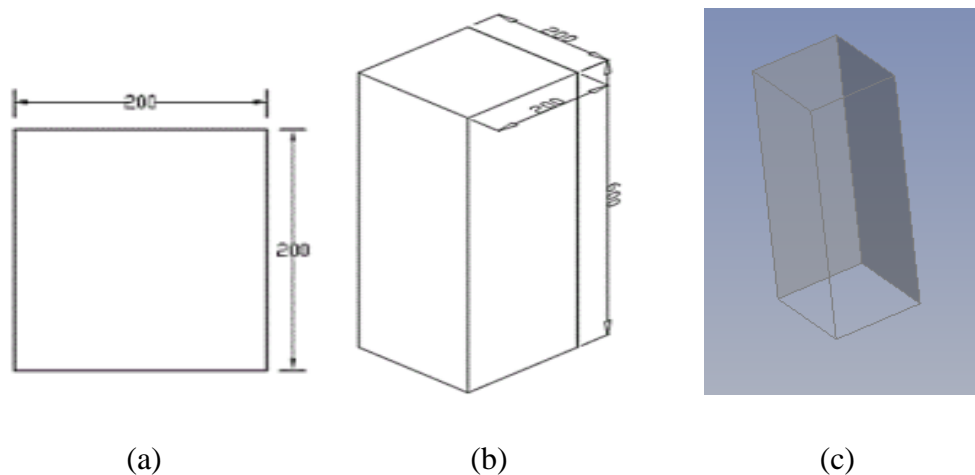


**Fig. 3.13 (a) Plan, (b) Elevation, & (c) Model of Square Validation model**

#### 3.5.1.2. Virtual Wind Tunnel (Domain)

Virtual Wind Tunnel is modeled w.r.t. the size and dimension of the building to be analyzed. General guideline for creating the model of the virtual wind tunnel or domain in the software follows that, if the building height is H, then the domain dimensions will be as  $20H*10H*6H$ , which will be distributed around the building model as shown in fig. 3.14.

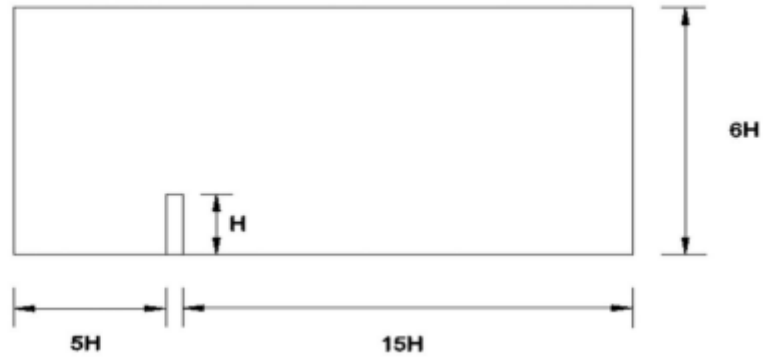


**Fig. 3.14 Dimensions of wind tunnel in side elevation**

As shown in the fig. 3.15 the dimensions of the wind tunnel are taken from the outside faces of the building.

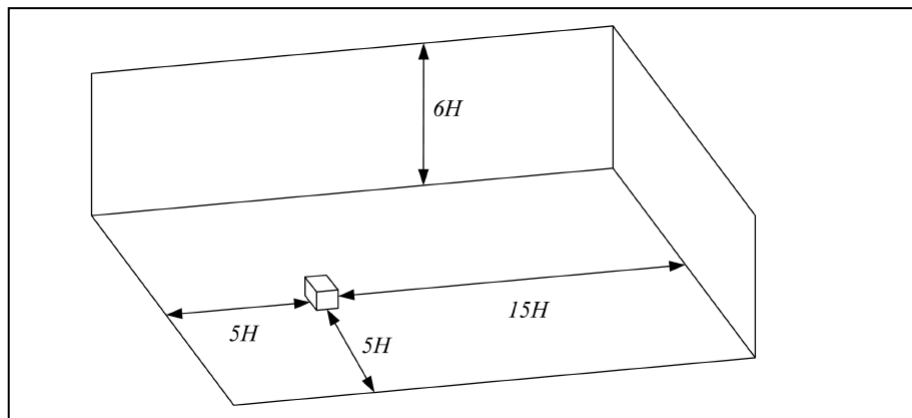


**Fig. 3.15 Dimension of the Domain in 3D view**

Geometry of the Domain made in Design modeler in Ansys CFX is shown in fig. 3.16, where the sample building inside the domain can be seen. The domain is made such a way so that win direction can be easily changed with different incident angle between wind and surface of the building model.

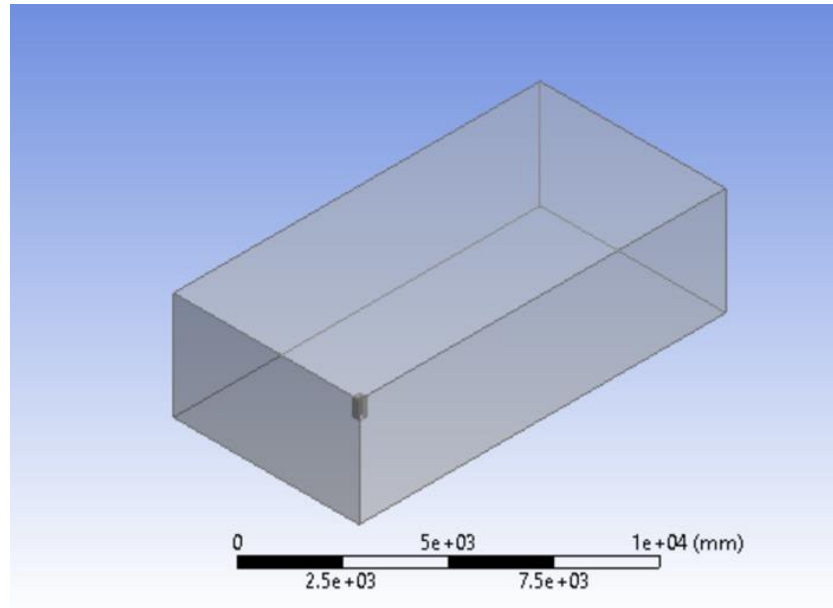


**Fig. 3.16 Wind Tunnel Domain in Ansys**

### 3.5.1.3. *Isolated Model*

For the study, the first model geometry to be made was H-Shaped High-rise building of 60m height scaled down to 600mm using the scale of 1:100.

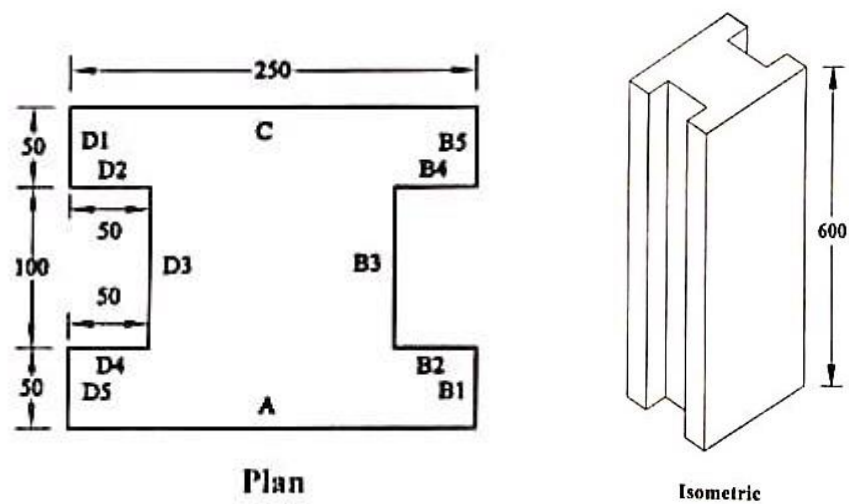


**Fig. 3.17 Plan and Isometric view of the H-shaped building**

Fig. 3.17 shows the plan and elevation for the H-shaped model for the isolated building study. This model is then placed in the virtual wind tunnel domain and then after applying the required wind flow through the domain, the flow characteristics and the building response is then evaluated as shown in fig. 3.18.

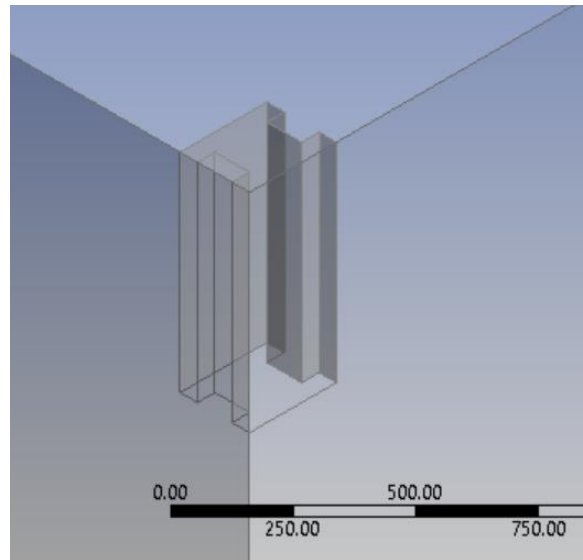


**Fig. 3.18 Isolated H-shaped Building model**

Since the model is symmetric in both X and Y, the incident angle to be changed to study the wind flow at different angles will vary from 0 to 90 degrees after which the results would repeat themselves.

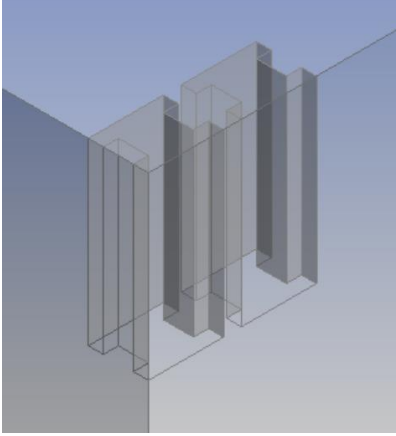
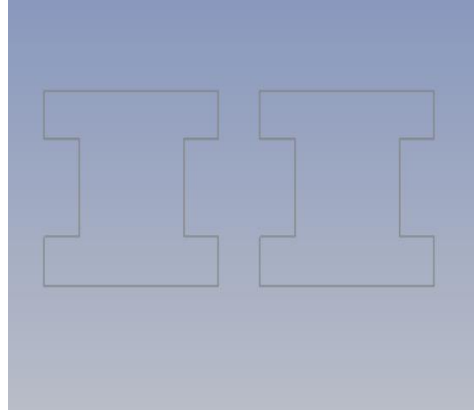
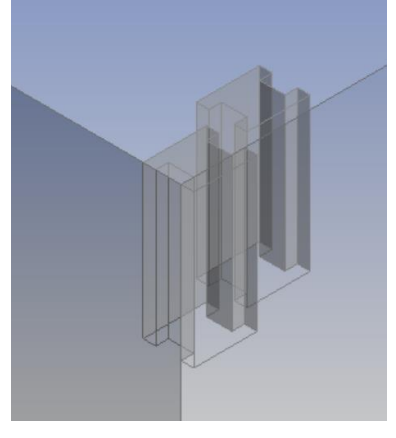
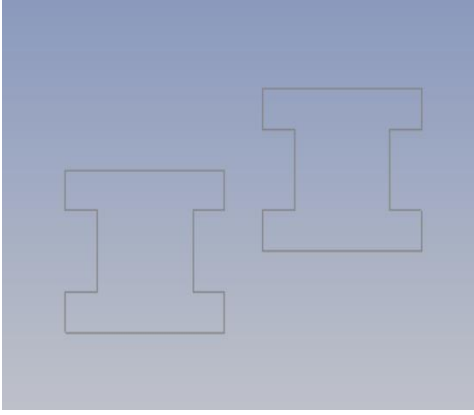
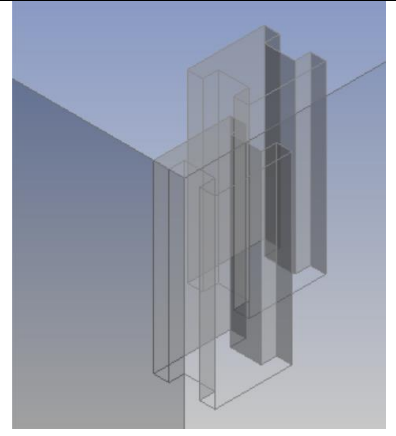
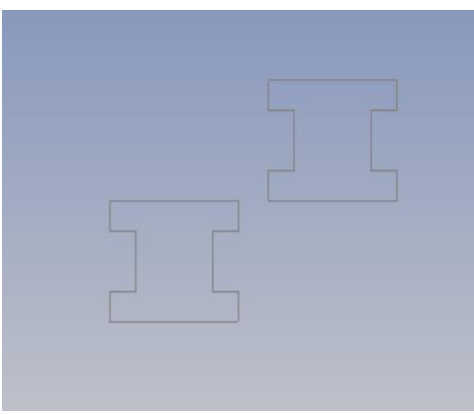
#### **3.5.1.4. Interference Model**

Interference study is done when either two or more than two bodies are exposed to the wind load then the effect of wind over the first building gets dependent on the simultaneous position of the other building/s.

In this study two identical H-shaped building of height 60m are modeled with scaled down to 600 mm and are exposed to the wind loading in the virtual wind tunnel domain.

Interference study is conducted in three different interfering configurations namely, Zero, Half, & Full interference condition, where the position of interfering building is changed w.r.t. the principal building as shown in table 3.1.

**Table 3.1 Three Interference Conditions of H-shaped building**

Full Interference		
Half Interference		
Zero Interference		

### 3.5.2. Meshing

Meshing is the process done in the process of software simulation in which the whole structure is divided into numerous small finite elements for the process of simulation. The size of the meshing can be changed as per our convenience, the smaller the size the accurate the results will be. To increase the precision the meshing for each element is done separately.

#### 3.5.2.1. Model Sizing Meshing

In this all meshing for the building model inside the domain is defined. The command used for meshing is called as Sizing. The size of the meshing chosen in this model is 0.008mm.

#### 3.5.2.2. Domain Sizing Meshing

For Domain i.e. Virtual wind tunnel, the ground meshing is done differently because the building model rests on this face. 'Sizing' command is used here too for defining the size of the meshing on the ground face of domain. Size used in domain is 0.08mm.

Fig. 3.19 shows the model after meshing is applied in both model and domain.

Meshing of the domain other than the ground is done by using the automatic default meshing provided by the Ansys CFX.

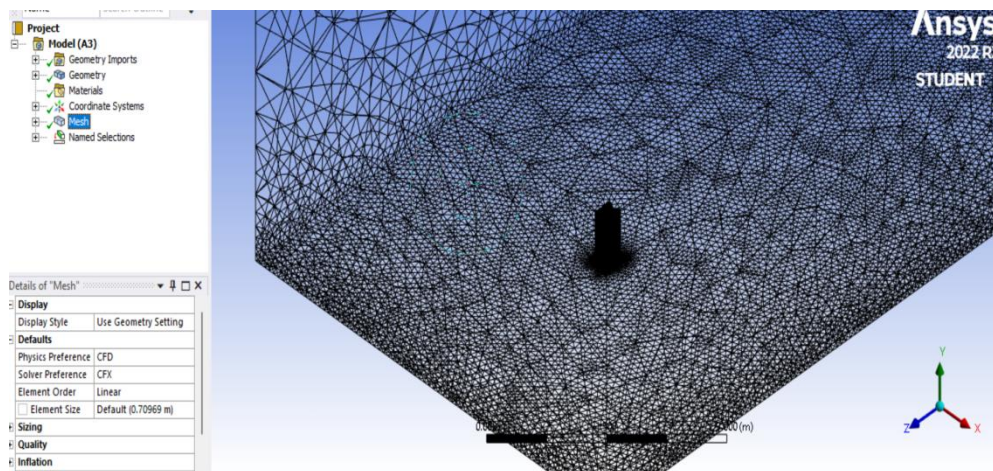


**Fig. 3.19 Model after meshing**



### 3.5.2.3. *Inflation Meshing*

Inflation meshing is provided when there is sudden change or irregularity in the geometry of the model. Hence, inflation meshing is provided in several layers to provide the smoothness in the analysis of the model.

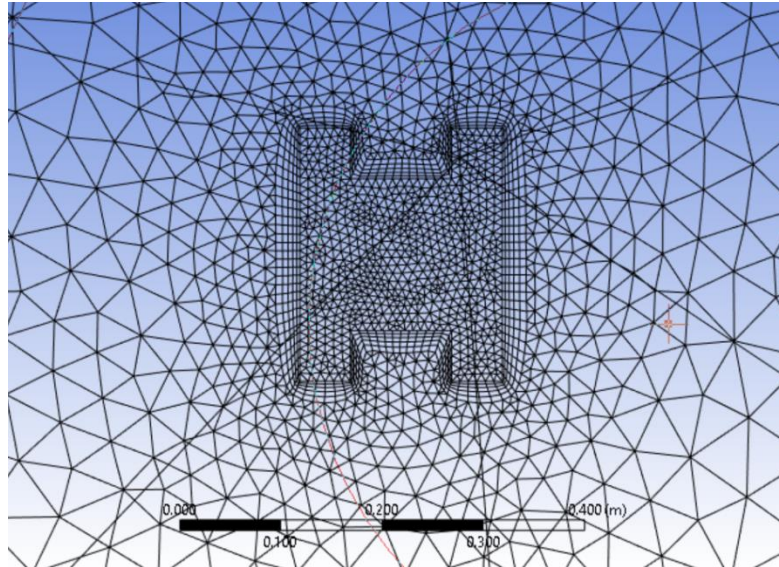


**Fig. 3.20 Inflation meshing**

Fig. 3.20 shows top view of the model building showing the inflation meshing in the model used at boundary of the building and then merging or small mesh of building into the bigger mesh of the domain throughout the several layers of inflation.

### 3.5.2.4. *Automatic Default Meshing*

Automatic Default Meshing is the meshing used for the parts of the model where any specific meshing is not needed.

After meshing is done naming of different faces of the building and domain is done for the setup and simulation of the model.

### **3.5.3. Setup and Boundary Conditions**

To complete the process of simulation of the models in each phases, i.e. validation, isolated and interference of the buildings, boundary conditions are defined and then mathematical equation are setup for the simulation of the model and analyze the buildings.

#### **3.5.3.1. *Boundary condition***

Simple boundary conditions are defined for the model to start the simulation of the building model.

##### *3.5.3.1.1. INLET of Domain*

Inlet is defined from where the wind starts to flow in to the virtual wind tunnel i.e. the domain. It is provided by providing the inlet wind velocity and its intensity through which it will be channeled into the domain over the building.

##### *3.5.3.1.2. OUTLET of Domain*

Outlet is defined by providing the output pressure to be 0 on the outlet face so that it creates a draft inside the domain like an actual wind tunnel where the wind comes from inlet and gets sucked out through the outlet.

##### *3.5.3.1.3. SIDE WALLS of Domain*

Side walls of the domain should behave like the walls of the actual wind tunnel hence are provided with the FREE SLIP property so that there is no penetration or friction from the walls that might affect the end result of the simulation.

#### 3.5.3.1.4. GROUND of Domain

The ground surface of the domain should be impenetrable for any wind to pass through so that wind effect can be fully examined over the building model. Hence, in the software itself the ground face of the domain the NO SLIP property is assigned for the ground.

Fig. 3.21 shows the model after boundary condition is applied. Arrow direction shows that the inlet and outlet of the domain are specified.

The total wind load is then applied on the inlet face by assigning the chosen mathematical equation for the simulation and solving purpose.

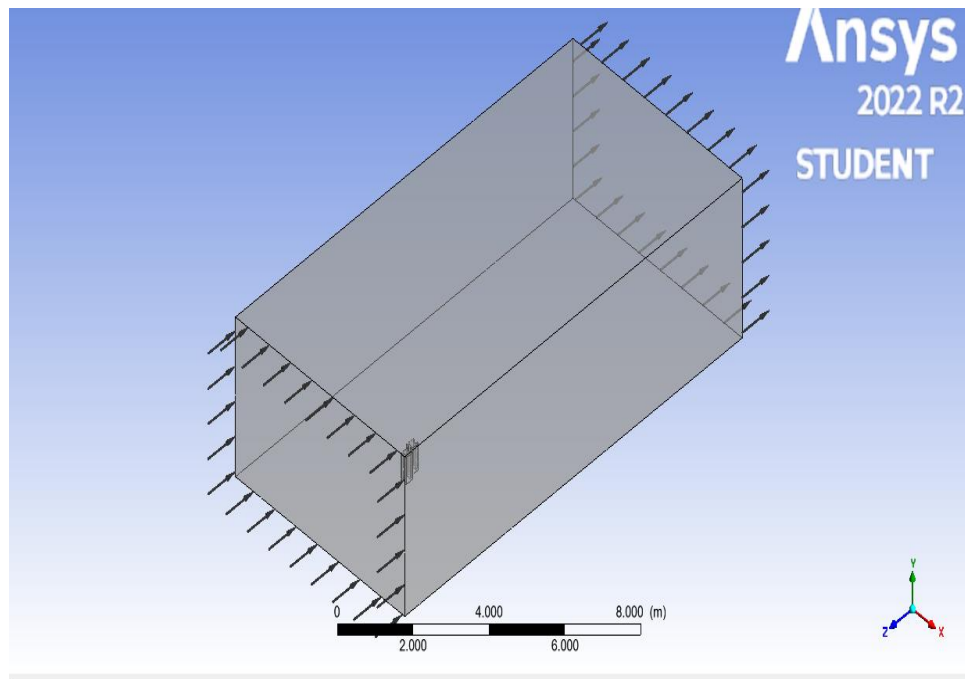


**Fig. 3.21 Model after Boundary condition are applied**

### 3.5.3.2. Setup for Simulation

Setup for the simulation is then provided by giving the chosen material properties (in this case ‘air’) and then numerical steps and precision for simulation and then entering the mathematical equation that will be used in the process.

The mathematical equation used is based on the empirical formula of the *Power Law*, already discussed in section 3.2.3 as equation (3.6). Equation setup in Ansys is shown in fig. 3.22.

Table 3.2 shows the input values for the setup.

**Table 3.2 Input Values used in Setup**

Reference Velocity, $U_{ref}$	10 m/s
Reference Height, $Z_{ref}$	1 m
Alpha, $\alpha$	0.145
Solver Control precision	$10^{-6}$
Air density, $\rho$	1.225 kg/m <sup>3</sup>

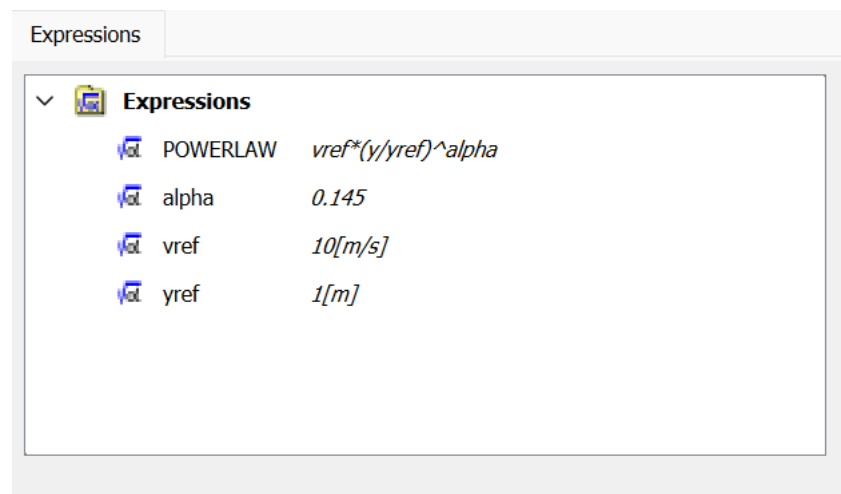


**Fig. 3.22 Equation setup in Ansys CFX**

The simulations are performed for each and every different incident angles between the wind and the building surface.

For Isolated building the variation of angles will be from 0 to 90 degrees with the simulations at every 15 degrees.

For Interference models the variation of angles will be from –

- 0 to 360 degrees for Zero and Half Interference with simulation after every 30 degrees.
- 0 to 180 degrees for Full Interference with simulation after every 30 degrees.

## **CHAPTER 4**

### **RESULTS AND DISCUSSIONS**

#### **4.1. GENERAL**

The outcomes of the experiment in the wind tunnel and the numerical simulations have been compared. It was seen that the CFD recreations were at standard with the standard results. Ansys provides various types of output data for deriving required comparative results.

#### **4.2. SIMULATION RESULTS**

After the simulation is complete Ansys gives the results in the form pressure contours, velocity flow line, pressure force values etc. to get more precise values the surface of the body can be marked by small elements to get values very close to each other and then by combining the values more accurate results can be inferred.

##### **4.2.1. Line method**

In this study pressure line method is used to get more accurate values of the wind pressure on the surfaces of the body. The whole body is divided into several pressure points. And then by joined two points that are in straight vertical line, two form lines throughout the body of the building.

Fig. 4.1 shows the marking of the pressure points on the H-shaped building and the corresponding pressure lines that are made on the H-shaped model.

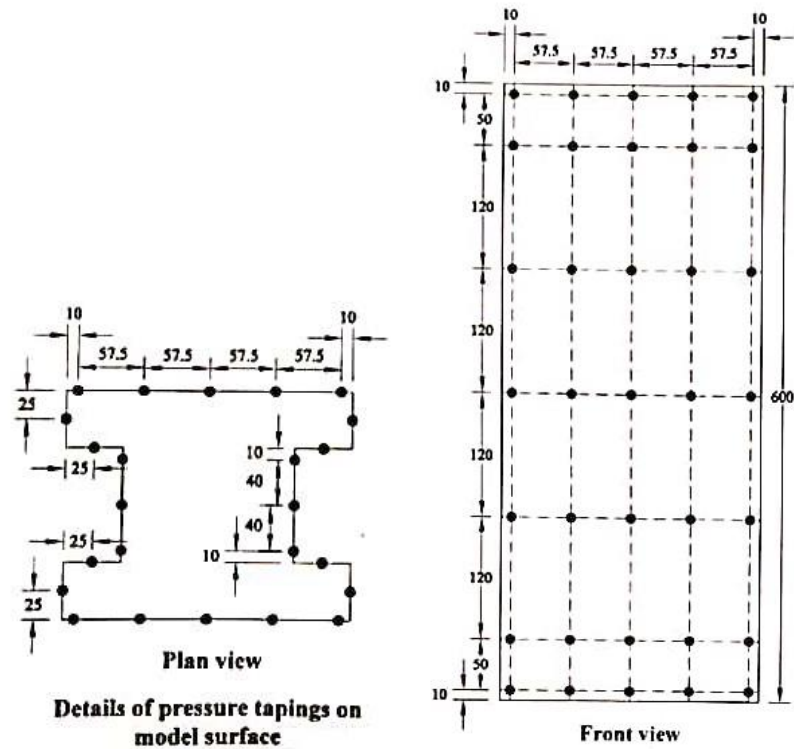


**Fig. 4.1 Pressure lines in H-shaped building**

Using this method resultant value can be taken on each of the lines such as pressure and forces etc.

#### 4.2.2. Pressure Contours

Pressure contours can be generated and their values can be exported for further analysis and deduction on the wind flow on the building.

Pressure contours give the values and variation of pressure over the entire building and where does the maximum and minimum pressure zones are being formed.

Pressure contours give both positive and negative values of the pressure showing that where the wind is pushing the building to generate positive pressure and where does suction formed which is resembled by the negative symbol of the pressure.

Fig. 4.2 shows a typical pressure contour diagram made in Ansys CFX. By using the line methods here we can find about the pressure on each line (shown in yellow color).

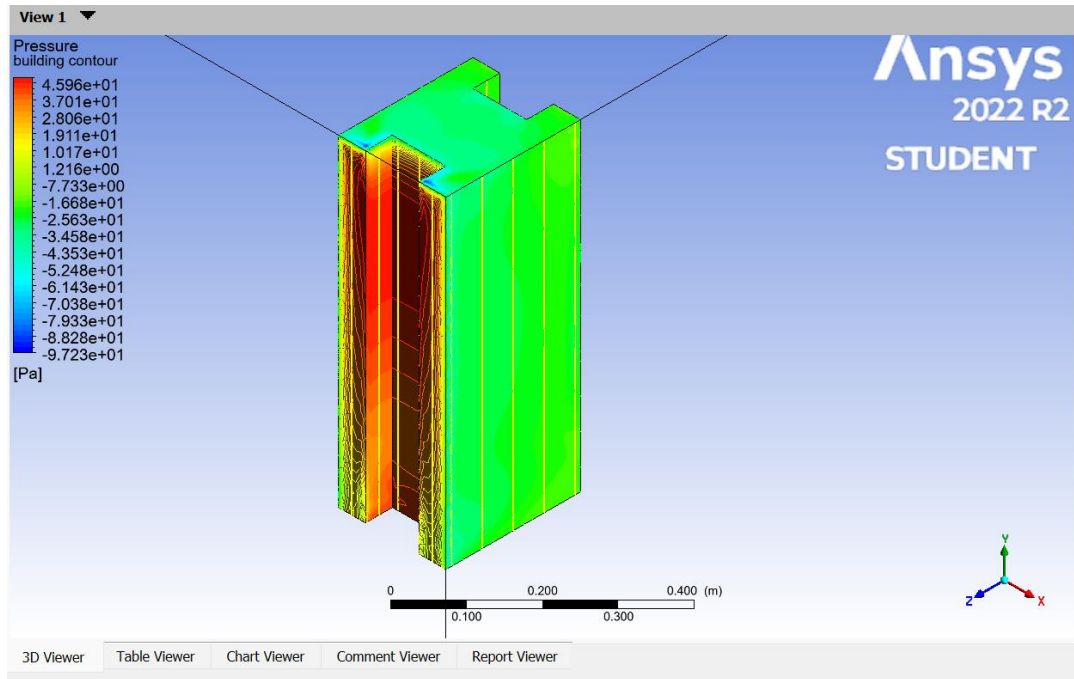


**Fig. 4.2 Typical pressure contour in ANSYS CFX**

### 4.2.3. Velocity Streamlines

Velocity Streamlines are formed to show the flow of the wind inside the domain and around the building.

Colors of the flow lines give the max and min values of the velocity. Pattern of the flow line shows how the flow of the wind gets changed near the building.

Fig. 4.3 shows a typical Velocity Streamline formed in Ansys.



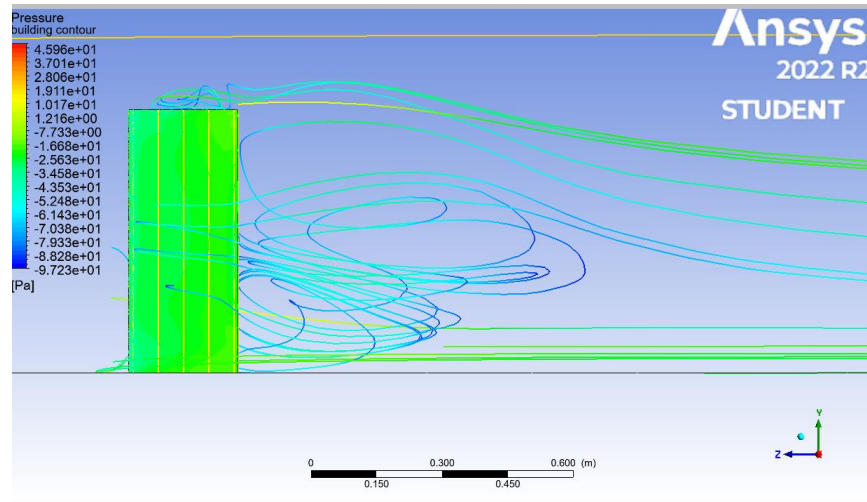


**Fig. 4.3 Typical Velocity streamline in Ansys**

#### 4.2.4. Coefficient of Pressure

According to fluid dynamics, pressure coefficient is a dimensionless number which portrays the overall pressure variation all through a flow region.

Coefficient of wind pressure can be calculated by the following relation.

$$C_p = \frac{P}{(0.5 * \rho_{air} * V_{ref}^2)} \quad (4.1)$$

Where,

Air density  $\rho_{air} = 1.225$

Reference velocity  $V_{ref} = 10$  m/s, at  $Z=1$  m

$P$  = Wind Pressure calculated

### 4.3. VALIDATION RESULTS

As per IS: 875 Part 3 (2015), IS code for wind load of structures, standard values for coefficient of pressure are being provided for some specified shapes of the objects when they are experimentally tested inside a wind tunnel.

Hence by simulating the similar model in Ansys and providing the similar wind loading conditions, validation of the virtual wind tunnel results can be done.

In this study, standard square shape building is modeled in Ansys to validate the work. The dimensions of the square model scaled down by 1:100 are 200mm\*200mm\*600mm. The model is then modeled and simulated in Ansys CFX and then the results were compared to that of IS: 875 Part 3 and some other standard codes.

Table 4.1 shows the compared results of the Coeff. of pressure  $C_p$  on the building's windward face along with some standard values of  $C_p$ .

**Table 4.1 Validation results of Square model**

Wind Loading Code	$C_p$ on Windward Face
By ANSYS CFX	0.78
ASCE 7-10	0.8
AS/NZS-1170.2(2002)	0.8
IS: 875 (Part3)(2015)	0.8

The results of the wind tunnel experiment and the numerical simulations have been compared. It was seen that the CFD recreations were at standard with the standard results in validation.

#### **4.4. ISOLATED STUDY**

Isolated H-shaped high-rise building was modeled for the study following the similar steps as that of the validation model.

Dimensions of the H-shaped building are shown in fig. 4.4 with the scale of 1:100. The respective wind tunnel domain was modeled.

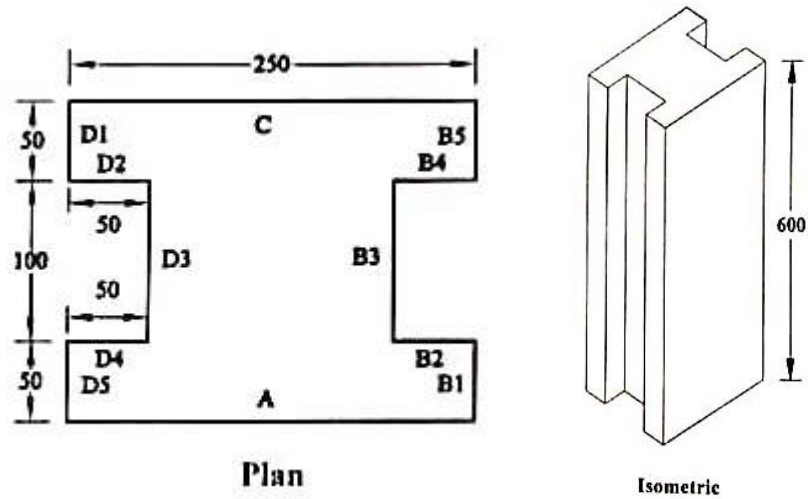


**Fig. 4.4 Plan and Isometric view of the H-shaped building**

- 3D isometric model and the domain made in Ansys are shown in fig. 4.5.

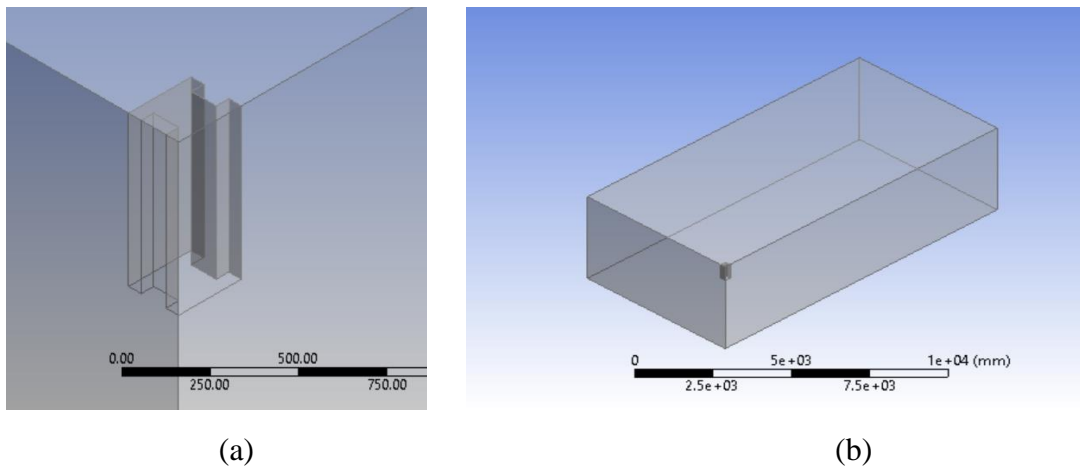


**Fig. 4.5 (a) H-shaped building model and (b) Domain in Ansys**

- Results are then accumulated in the form of pressure contours, velocity streamlines, coefficient of pressure, max & min wind pressure.

## Pressure contour, Velocity Streamline, Coefficient of Pressure

- Pressure contour for the isolated H-shaped model are as shown in the fig. 4.6 & fig. 4.7.

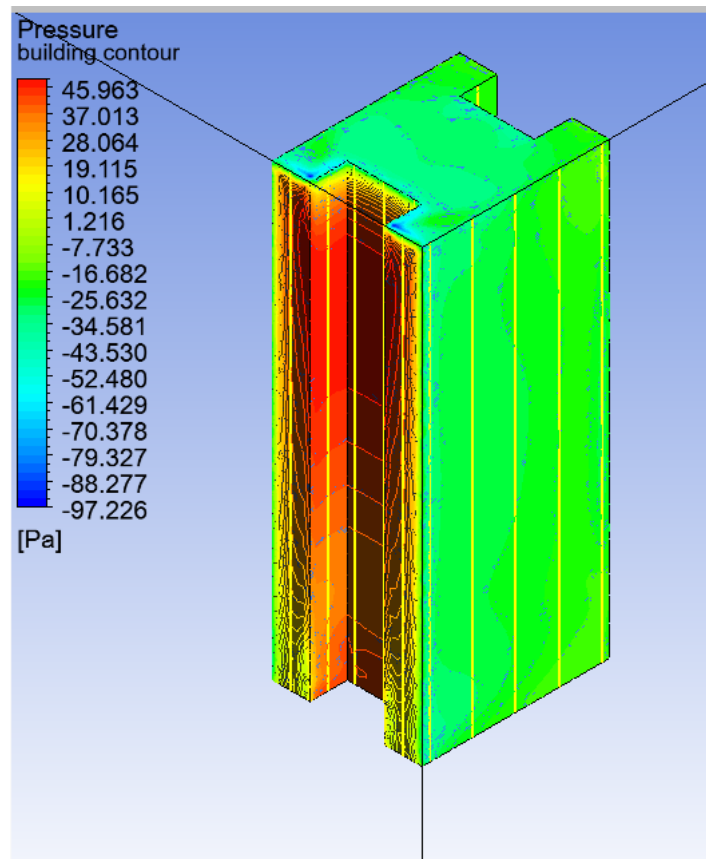


Fig. 4.6 Pressure Contour of the Isolated H-shaped model

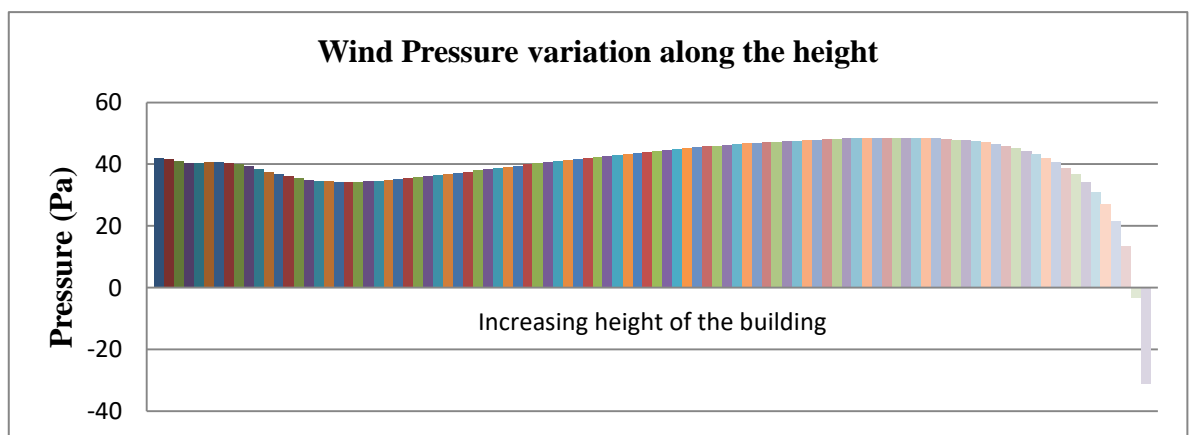
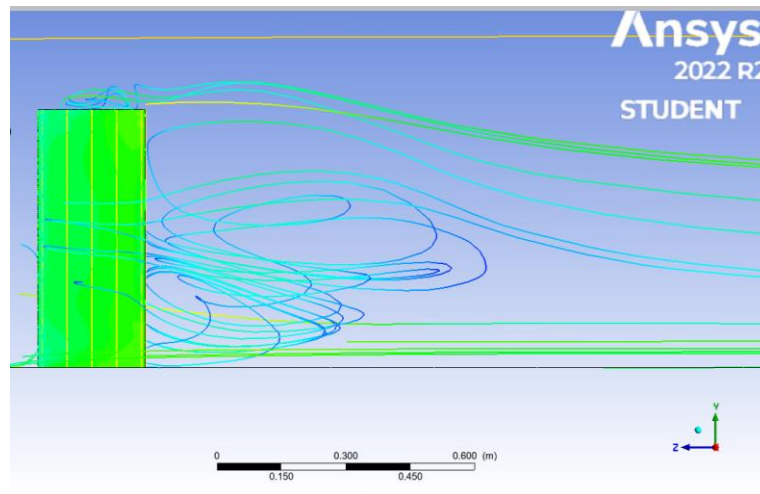


Fig. 4.7 Variation of Pressure with the increasing height of the building

- Velocity Stream line diagram obtained from Ansys for isolated H-shaped building is shown in fig. 4.8.



**Fig. 4.8 Velocity Streamline for Isolated H-shaped building**

- Coefficient of pressure over the height on the windward face of H-shaped building model is plotted in fig. 4.9.

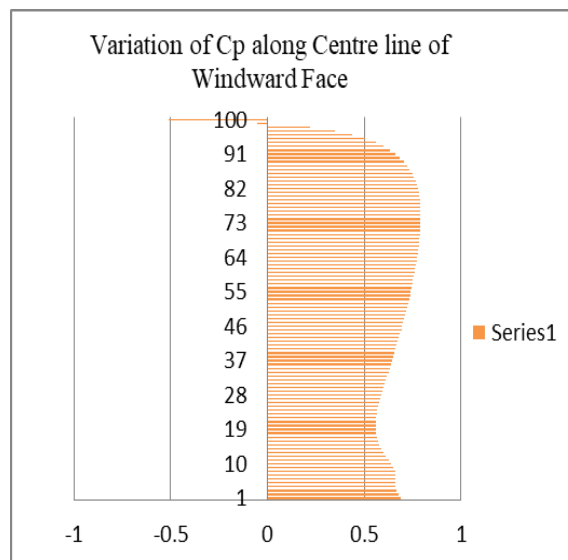


**Fig. 4.9 Variation Cp along the height of the building**

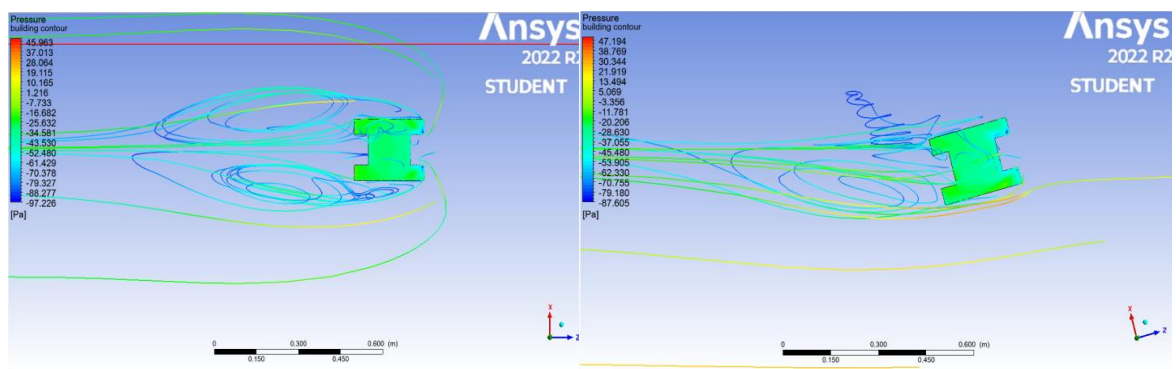
- Average Coefficient of wind Pressure on the windward face of the H-shaped building was found to be **0.6554**.
- Average Wind pressure on the windward face of the building was **40.1428 Pa**

#### 4.4.1. Effect of Wind incident angle

Wind is a very unpredictable phenomenon when it comes to the direction of loading. Hence, when wind loading is concerned, it is necessary to do the analysis of wind loading from all directions. In this study for isolated H-shaped building, since it is symmetric in both x and y directions then we do not need to change the incident wind angle from 0 to 360 degrees.

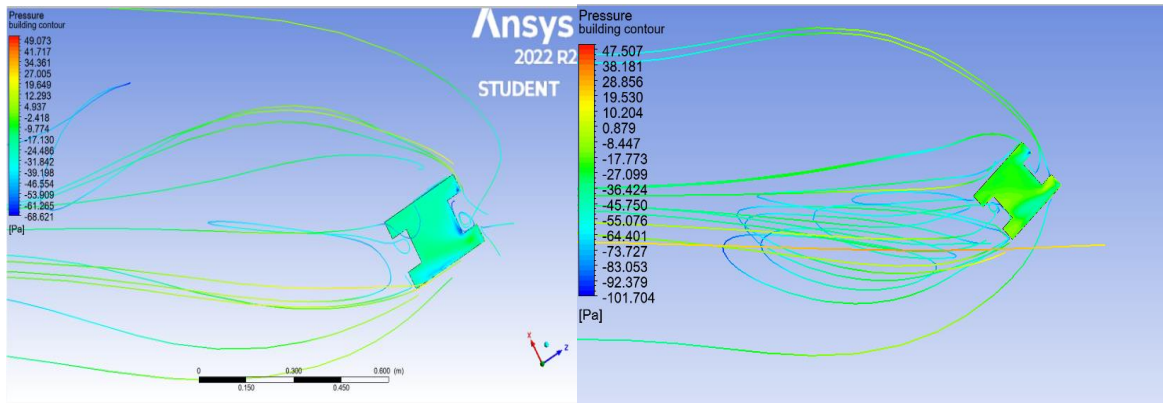
Here, the variation of incident angles was taken from 0 to 90 degrees because after that the result values will start repeating as shown in fig. 4.10.

To change the incident angles of the wind, the whole domain is being rotated from 0 to 90°.



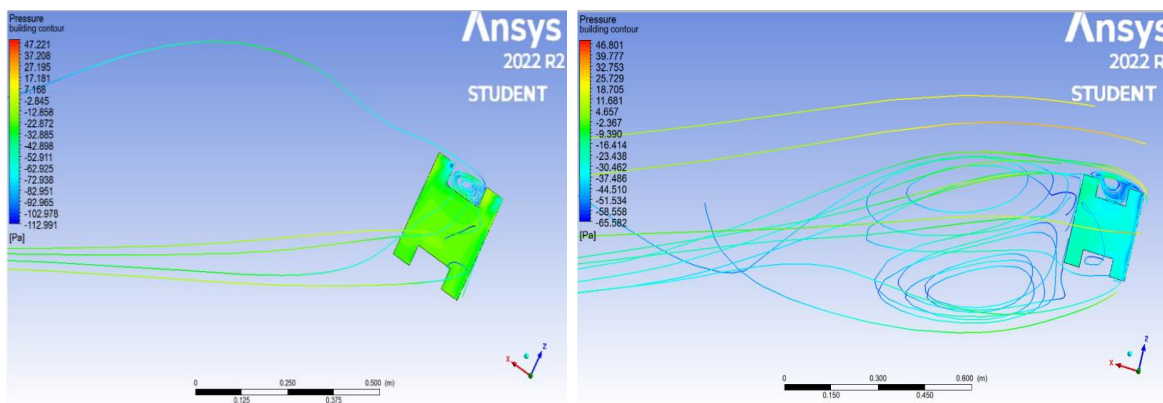
(a) 0 degrees

(b) degrees



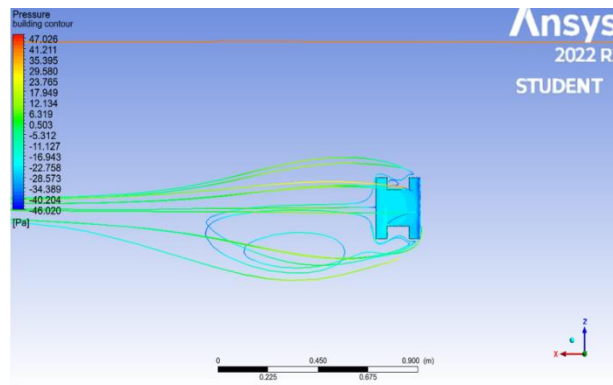
(c) 30 degrees

(d) 45 degrees



(e) 60 degrees

(f) 75 degrees



(g) 90 degrees

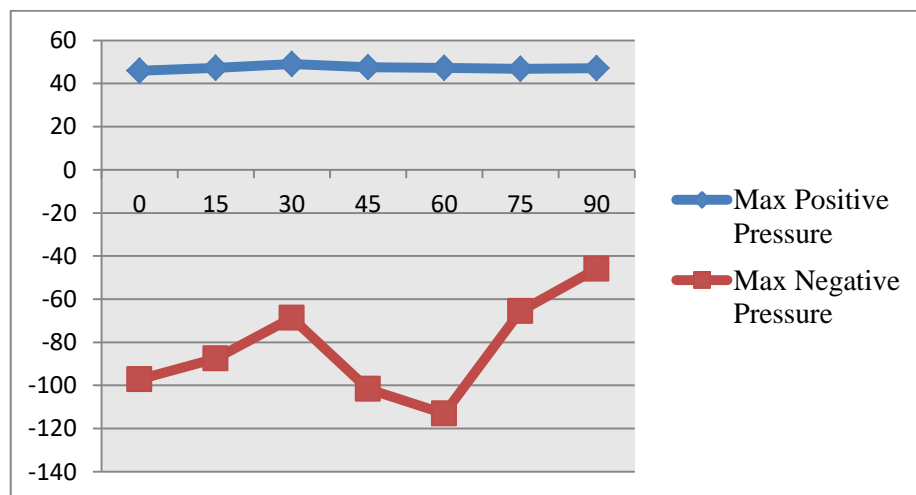
**Fig. 4.10 Pressure contour and Velocity streamlines at different angles of incidence**

Fig. 4.9 also shows the different pressure contours and velocity streamlines of the H-shaped model at different wind incident angles.

On comparing the result of each angle, table 4.2 shows the max positive and max negative wind pressure and the corresponding comparative graph is shown in fig. 4.11.

**Table 4.2 Average Pressure at Different Wind Incidence angles**

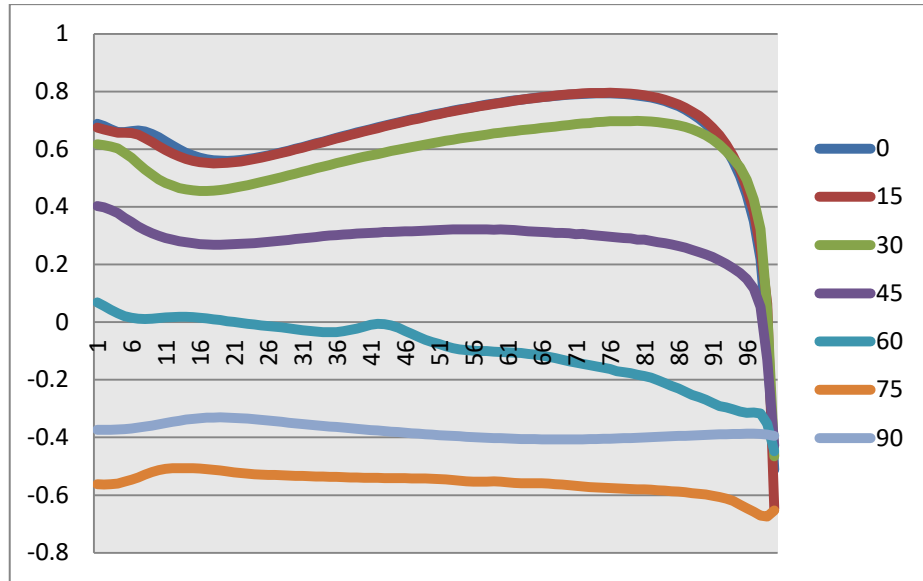
Angle of Incidence	Max Positive Pressure	Max Negative Pressure
0	45.963	-97.226
15	47.194	-87.605
30	49.073	-68.621
45	47.507	-101.704
60	47.221	-112.991
75	46.801	-65.582
90	47.026	-46.02



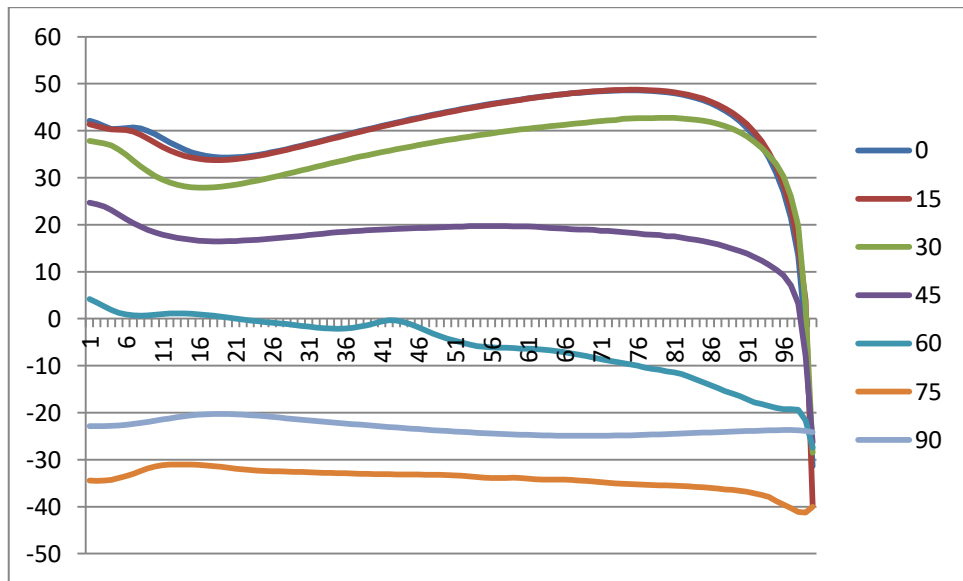
**Fig. 4.11 Graphical comparison of max wind pressure at different angles**

Fig. 4.12 consists of the charts showing the graphical comparison between the wind pressure and the coefficient of wind pressure at different wind incident angles.





(a)  $C_p$  at different angles for Isolated H-shaped building



(b) Comparison of Wind Pressure at different incident angles

Fig. 4.12 (a)  $C_p$  (b) Wind pressure at different wind incident angles along the height of the model

## 4.5. INTERFERENCE STUDY

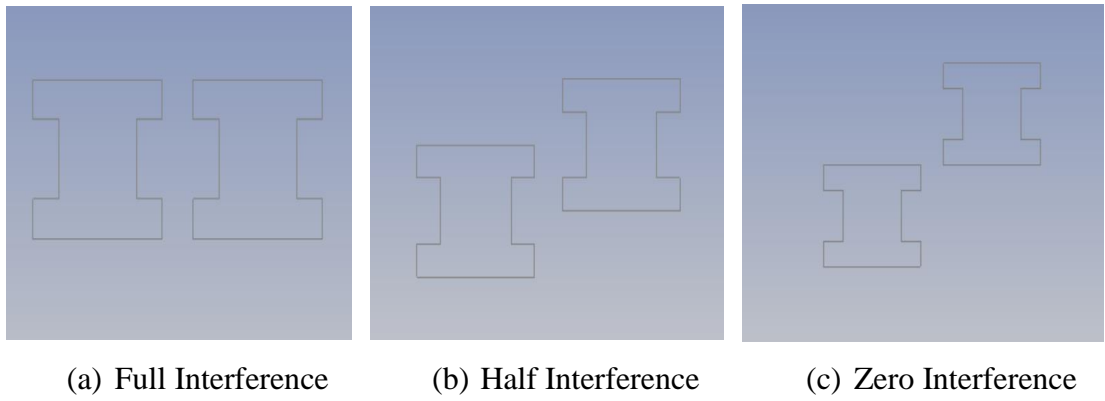
Interference effect in wind flow characteristics comes into play when there is more than one body under the same wind flow draft. Then the wind flow characteristics around the main principal building (PB) are affected by the interfering building (IB).

In this study, the interfering effect was studied between two identical H-shaped buildings of height 60m each modeled scaled down to 600mm height by a scale of 1:100, in Ansys CFX.

Three types of interference are performed depending on the position of the IB w.r.t. the PB, namely, FULL, HALF and Zero interference, where the position of the PB was fixed near the origin but the position of the IB was different w.r.t. the PB and origin with a min distance of 10% of the height of the building between them.

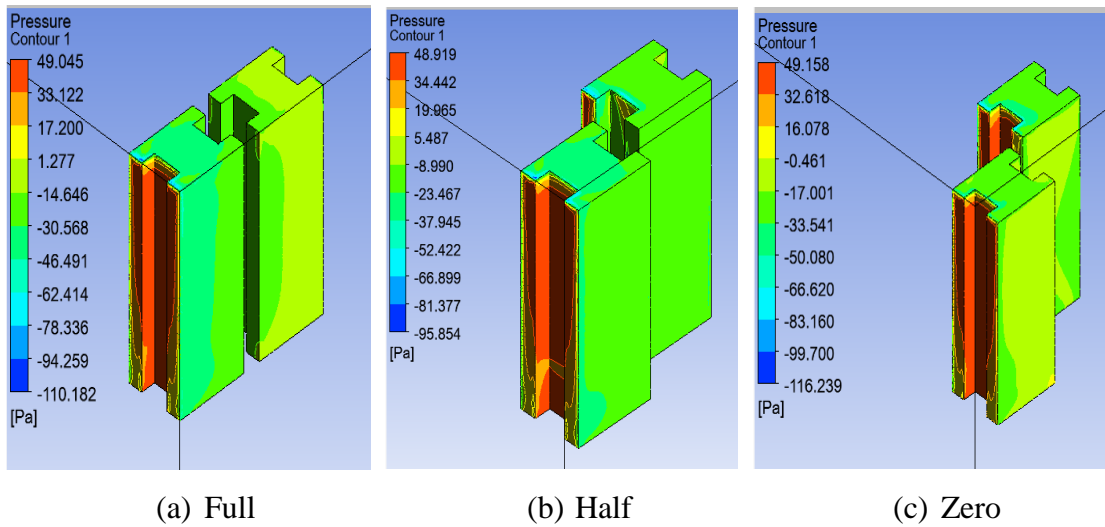
- For Full interference, the IB should be directly behind the PB so the whole IB is behind PB.
- For Half interference, the one end face IB start from the mid-section of the PB i.e. from origin axis, leaving half of IB behind PB.
- For Zero interference, the IB should start from the end face of the PB so that no part of IB should be present behind the PB.

Fig. 4.13 shows the interference configurations of the model.



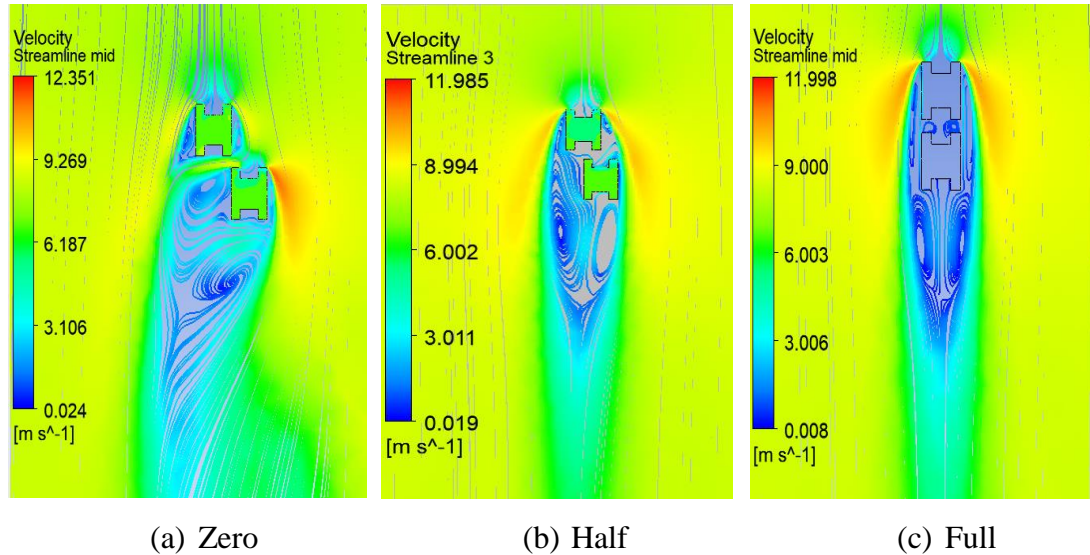
**Fig. 4.13 Interference between two H-shaped buildings**

Fig. 4.14 consists of several pressure contours taken after simulations were performed for the three interference conditions.



**Fig. 4.14 Pressure contours for interference conditions in H-shaped buildings**

Fig. 4.15 consists of the velocity streamlines of the different interference conditions of the H-shaped building models.



**Fig. 4.15 Velocity Streamlines for interference conditions oh H-shaped buildings**

#### 4.5.1. Effect of Wind incidence angles

Interference models were then analyzed for different wind incidence angles between the two building models and the virtual wind tunnel domain from 0 to 360 degrees.

Results of different wind incidence angle from Ansys were then compared to get a comparative result between the different wind incident angles in terms of wind pressure.

Max positive and max negative wind pressures were then found and compared for each wind incidence angles and a graphical comparison was done among them.

- For max positive wind pressure, table 4.3 consists of the values for the max positive wind pressure and their graphical representation is shown in fig. 4.16.

**Table 4.3 Maximum Positive Wind pressure (Pa) at different angles in interference**

Angle of Incidence	Zero Interference	Half Interference	Full Interference
0	49.158	48.919	49.045
30	50.838	51.728	52.485
60	49.813	48.498	50.788
90	48.567	48.204	48.145
120	50.484	49.357	52.485
150	52.117	52.256	50.788
180	53.626	48.97	48.145
210	50.925	51.539	52.485
240	49.859	49.754	50.788
270	48.725	48.113	48.145
300	50.194	49.568	52.485
330	52.194	52.4	50.788
360	49.158	48.919	49.045

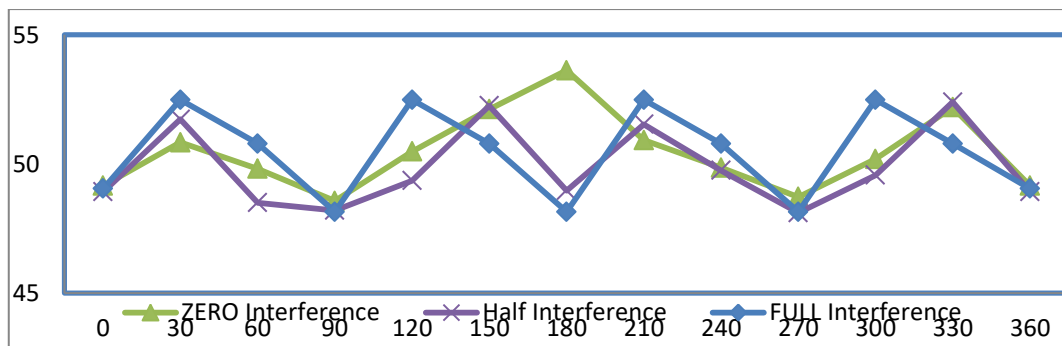


**Fig. 4.16 Graphical representation of Max Wind pressure at different angles in Interference**

- For max negative wind pressure, table 4.4 consists of the values for the max positive wind pressure and their graphical representation is shown in fig. 4.17.

**Table 4.4 Maximum Negative Wind pressure (Pa) at different angles in interference**

Angle of Incidence	Zero Interference	Half Interference	Full Interference
0	116.239	95.854	110.182
30	128.48	125.16	102.546
60	131.636	129.828	140.371
90	96.322	116.158	92.398
120	104.598	87.504	102.546
150	116.182	119.473	140.371
180	129.329	97.348	92.398
210	116.334	126.541	102.546
240	131.93	118.067	140.371
270	94.59	98.679	92.398
300	114.757	117.854	102.546
330	118.996	130.507	140.371
360	116.24	95.854	110.182

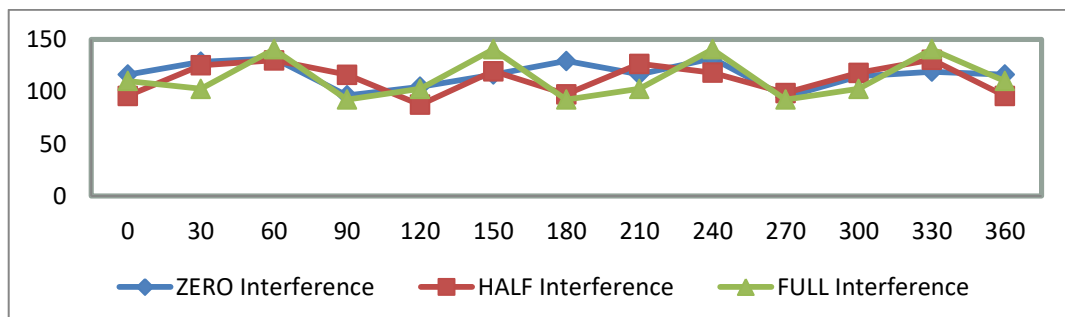


**Fig. 4.17 Graphical representation of Max Wind pressure at different angles in Interference**

## CHAPTER 5

### CONCLUSION

This study is performed to investigate the wind flow characteristics on a high-rise building for the response of the tall buildings against the high velocity wind loads. Wind is an unpredictable phenomenon which varies in both time and space. Generally, the tall buildings are constantly under the effect of the wind pressure from every direction. In this study a 60m tall H-shaped high-rise building was modeled using ANSYS CFX for a coastal region where the wind velocity is quite high. Detailed literature review has been done in order to grasp the knowledge on the area. First, validation of work was done by simulating a standard 200mm\*200mm square model as per IS: 875 Part 3(2015), for wind load. Later the H-shaped building with plan area of about 40000mm<sup>2</sup> was modeled for both Isolated and Interference conditions and the results were then drawn from Ansys.

Following are the conclusions from the study –

- ANSYS CFX provides pressure experiences and flow patterns as well. Flow patterns provided information about vortex formation and flow separation in the negative pressure zone.
- It was discovered that each building's windward face had the greatest positive pressure because of direct wind contact.
- Because of the production of vortices, the strain coefficient for the side essences of each building was more negative than the tension coefficient for the back faces.

- Due to Symmetry of the structure similar results were obtained after each 90° rotation of the building with respect to the lateral wind loading in the virtual tunnel formed in ANSYS CFX.
- Velocity of wind across the building modelled are provided through the Velocity Stream lines in ANSYS CFX post processing.
- On comparing with the standard Square model, “H” plan shaped building is subjected to a higher pressure than the square Model.



## REFERENCES

1. P. A. Irwin, “Bluff body aerodynamics in wind engineering,” *Journal of Wind Engineering and Industrial Aerodynamics*, vol. 96, no. 6–7, pp. 701–712, Jun. 2008, doi: <https://doi.org/10.1016/j.jweia.2007.06.008>.
2. A.Khalilzadeh, H. Ge, and H. D. Ng, “Effect of turbulence modeling schemes on wind-driven rain deposition on a mid-rise building: CFD modeling and validation,” *Journal of Wind Engineering and Industrial Aerodynamics*, vol. 184, pp. 362–377, Jan. 2019, doi: <https://doi.org/10.1016/j.jweia.2018.11.012>.
3. Y. Wang and X. Chen, “Evaluation of wind loads on high-rise buildings at various angles of attack by wall-modeled large-eddy simulation,” *Journal of Wind Engineering and Industrial Aerodynamics*, vol. 229, p. 105160, Oct. 2022, doi: <https://doi.org/10.1016/j.jweia.2022.105160>.
4. C. Zheng, Y. Xie, M. Khan, Y. Wu, and J. Liu, “Wind-induced responses of tall buildings under combined aerodynamic control,” *Engineering Structures*, vol. 175, pp. 86–100, Nov. 2018, doi: <https://doi.org/10.1016/j.engstruct.2018.08.031>.
5. B. Yang, H. Zhu, Q.-L. Zhang, R. Wüchner, S. Sun, and J. Qiu, “Identification of wind loads on a 600 m high skyscraper by Kalman filter,” vol. 63, pp. 105440–105440, Oct. 2022, doi: <https://doi.org/10.1016/j.jobe.2022.105440>.
6. J. Shanmugasundaram, S. Arunachalam, S. Gomathinayagam, N. Lakshmanan, and P. Harikrishna, “Cyclone damage to buildings and structures — a case study,” *Journal of Wind Engineering and Industrial Aerodynamics*, vol. 84, no. 3, pp. 369–380, Feb. 2000, doi: [https://doi.org/10.1016/S0167-6105\(99\)00114-2](https://doi.org/10.1016/S0167-6105(99)00114-2).

7. A.Rukhaiyar, B. Jayant, K. Dahiya, R. K. Meena, and R. Raj, “CFD simulations for evaluating the wind effects on high-rise buildings having varying cross-sectional shape,” *Journal of Structural Fire Engineering*, Aug. 2022, doi: <https://doi.org/10.1108/jsfe-04-2022-0016>.
8. Nagar SK, Raj R, and Dev N, “Experimental study of wind-induced pressures on tall buildings of different shapes,” *Wind Struct Int J*, no. 31(5), pp. 441–453, 2020, Available: <https://doi.org/10.12989/was.2020.31.%205.431>.
9. S. Verma, R. Panneer Selvam, Z. Tang, and D. Zuo, “Comparison of Tornado-induced pressures on building from CFD model with TTU experimental measurements,” *Journal of Wind Engineering and Industrial Aerodynamics*, vol. 228, p. 105076, Sep. 2022, doi: <https://doi.org/10.1016/j.jweia.2022.105076>.
10. Y. Hu, Y. Peng, Z. Gao, and F. Xu, “Application of CFD plug-ins integrated into urban and building design platforms for performance simulations: A literature review,” *Frontiers of Architectural Research*, Jul. 2022, doi: <https://doi.org/10.1016/j.foar.2022.06.005>.
11. Anoop Kodakkal *et al.*, “Risk-averse design of tall buildings for uncertain wind conditions,” vol. 402, pp. 115371–115371, Sep. 2022, doi: <https://doi.org/10.1016/j.cma.2022.115371>.
12. P. A. BLACKMORE, “THE ROLE OF WIND TUNNEL TESTING IN THE DESIGN OF BUILDING STRUCTURES.,” *Proceedings of the Institution of Civil Engineers - Structures and Buildings*, vol. 122, no. 3, pp. 253–265, Aug. 1997, doi: <https://doi.org/10.1680/istbu.1997.29797>.
13. H. Tanaka, Y. Tamura, K. Ohtake, M. Nakai, and Y. Chul Kim, “Experimental investigation of aerodynamic forces and wind pressures acting on tall buildings with various unconventional configurations,” *Journal of Wind Engineering and Industrial Aerodynamics*, vol. 107–108, pp. 179–191, Aug. 2012, doi: <https://doi.org/10.1016/j.jweia.2012.04.014>.

14. B. Bhattacharyya and Sujit Kumar Dalui, "Investigation of mean wind pressures on 'E' plan shaped tall building," vol. 26, no. 2, p. 99, Feb. 2018, doi: <https://doi.org/10.12989/was.2018.26.2.099>.
15. S. Adhikari, Sujit Kumar Dalui, and A. Ahuja, "Experimental Investigation of Surface Pressure on '+' Plan Shape Tall Building," vol. 8, no. 3, Jan. 2014.
16. L. Carassale, A. Freda, and Michela Marrè-Brunenghi, "Experimental investigation on the aerodynamic behavior of square cylinders with rounded corners," vol. 44, pp. 195–204, Jan. 2014, doi: <https://doi.org/10.1016/j.jfluidstructs.2013.10.010>.
17. E. K. Bandi, Y. Tamura, A. Yoshida, Y. Chul Kim, and Q. Yang, "Experimental investigation on aerodynamic characteristics of various triangular-section high-rise buildings," *Journal of Wind Engineering and Industrial Aerodynamics*, vol. 122, pp. 60–68, Nov. 2013, doi: <https://doi.org/10.1016/j.jweia.2013.07.002>.
18. S. Pal, R. Raj, and S. Anbukumar, "Bilateral Interference of Wind Loads Induced on Duplicate Building Models of Various Shapes," *Latin American Journal of Solids and Structures*, vol. 18, no. 5, 2021, doi: <https://doi.org/10.1590/1679-78256595>.
19. R. Raj, T. Rana, and U. Khola, "Numerical study of wind excited action on H Plan-shaped tall building," *Int. J. Emerg. Technol*, no. 11 (3), pp. 591–605, 2020.
20. S. Hajra and S.K. Dalui, "Numerical investigation of interference effect on octagonal plan shaped tall buildings," *Jordan J. Civ. Eng*, no. 10 (4), pp. 462–479, 2016.
21. R. K. Meena, R. Raj, and S. Anbukumar, "Wind Excited Action around Tall Building Having Different Corner Configurations," *Advances in Civil Engineering*, vol. 2022, pp. 1–17, Feb. 2022, doi: <https://doi.org/10.1155/2022/1529416>.

22. A.Kumar and R. Raj, “CFD Study of Flow Characteristics and Pressure Distribution on Re-Entrant Wing Faces of L-Shape Buildings,” vol. 10, no. 1, pp. 289–304, Jan. 2022, doi: <https://doi.org/10.13189/cea.2022.100125>.
23. J. Amin and A. Ahuja, “Experimental study of wind-induced pressures on buildings of various geometries,” *International Journal of Engineering, Science and Technology*, vol. 3, no. 5, Aug. 2011, doi: <https://doi.org/10.4314/ijest.v3i5.68562>.
24. P. K. Goyal, S. Kumari, S. Singh, R. K. Saroj, R. K. Meena, and R. Raj, “Numerical Study of Wind Loads on Y Plan-Shaped Tall Building Using CFD,” *Civil Engineering Journal*, vol. 8, no. 2, pp. 263–277, Feb. 2022, doi: <https://doi.org/10.28991/cej-2022-08-02-06>.
25. A.Verma, R. K. Meena, H. Dubey, R. Raj, and S. Anbukumar, “Wind Effects on Rectangular and Triaxial Symmetrical Tall Building Having Equal Area and Height,” *Complexity*, vol. 2022, pp. 1–20, Jul. 2022, doi: <https://doi.org/10.1155/2022/4815623>.
26. J. D. Holmes, *Wind Loading of Structures*. CRC Press, 2018.
27. Standards Australia Limited and Standards New Zealand, *Structural design actions. Part 2, Wind actions*. Sydney, Nsw: Sai Global Limited Under Licence From Standards Australia Limited; Wellington, 2011.
28. Bureau of Indian Standards, *IS 875.3: Code of Practice for Design Loads (Other than Earthquake) for Buildings and Structures - Part 3: Wind Loads (IS 875 : Part 3) + Amendment 2016*. 2015. Accessed: May 23, 2023. [Online]. Available: <https://archive.org/details/gov.in.is.875.3.2015>
29. J. Revuz, D. M. Hargreaves, and J. S. Owen, “On the domain size for the steady-state CFD modelling of a tall building,” *Wind and Structures*, vol. 15, no. 4, pp. 313–329, Jul. 2012, doi: <https://doi.org/10.12989/was.2012.15.4.313>.

## **LIST OF PUBLICATIONS**

- [1]CFD Analysis for Wind Flow Characteristics of Various Facades in a High-Rise Building Using ANSYS CFX, (IKDSAK, 2023 – Scopus Index Conference, IITM, Janakpuri, Delhi).
- [2]CFD study Interference effect between Two H-Shaped tall buildings under bilateral wind induced loads using ANSYS CFX, (MMSPS, 2023 – Scopus Indexed, NIT Surat)(Accepted).